Biological Journal of the Linnean Society, 2021, **XX**, 1–24. With 4 figures.

Species diversity and biogeography of an ancient frog clade from the Guiana Shield (Anura: Microhylidae: *Adelastes*, *Otophryne*, *Synapturanus*) exhibiting spectacular phenotypic diversification

ANTOINE FOUQUET[1,*], KILLIAN LEBLANC[1], MARLENE FRAMIT[1], ALEXANDRE RÉJAUD[1], MIGUEL T. RODRIGUES[2], SANTIAGO CASTROVIEJO-FISHER[3], PEDRO L. V. PELOSO[4], IVAN PRATES[5], SOPHIE MANZI[1], UXUE SUESCUN[1], SABRINA BARONI[2], LEANDRO J. C. L. MORAES[6], RENATO RECODER[2], SERGIO MARQUES DE SOUZA[2], FRANCISCO DAL VECCHIO[2], AGUSTÍN CAMACHO[2], JOSÉ MARIO GHELLERE[3], FERNANDO J. M. ROJAS-RUNJAIC[3,7], GIUSSEPE GAGLIARDI-URRUTIA[3,8], VINÍCIUS TADEU DE CARVALHO[9], MARCELO GORDO[10], MARCELO MENIN[10], PHILIPPE J. R. KOK[11], TOMAS HRBEK[12], FERNANDA P. WERNECK[6], ANDREW J. CRAWFORD[13], SANTIAGO R. RON[14], JONH JAIRO MUESES-CISNEROS[15], ROMMEL ROBERTO ROJAS ZAMORA[10], DANTE PAVAN[16], PEDRO IVO SIMÕES[17], RAFFAEL ERNST[18] and ANNE-CLAIRE FABRE[19,20]

[1]*Laboratoire Evolution et Diversité Biologique, UMR 5174, CNRS, IRD, Université Paul Sabatier, Bâtiment 4R1 31062 cedex 9, 118 Route de Narbonne, 31077 Toulouse, France*
[2]*Universidade de São Paulo Instituto de Biociências, Departamento de Zoologia, São Paulo, SP, Brazil*
[3]*Pontifícia Universidade Católica do Rio Grande do Sul, Laboratório de Sistemática de Vertebrados / Programa de Pós-Graduação em Ecologia e Evolução da Biodiversidade, Escola de Ciências da Saúde e da Vida, Porto Alegre, RS, Brazil*
[4]*Universidade Federal do Pará, Instituto de Ciências Biológicas, R. Augusto Corrêa, 1, Guamá, Belém, 66075-110, Pará, Brazil*
[5]*Department of Ecology and Evolutionary Biology, University of Michigan, Ann Arbor, MI, USA*
[6]*Instituto Nacional de Pesquisas da Amazônia, Coordenação de Biodiversidade, Avenida André Araújo 2936, 69080-971, Manaus, AM, Brazil*
[7]*Fundación La Salle de Ciencias Naturales, Museo de Historia Natural La Salle, Sección de Herpetología, Caracas 1050, Venezuela*
[8]*Peruvian Center for Biodiversity and Conservation (PCB&C), Iquitos, Peru*
[9]*Programa de Pós-Graduação em Diversidade Biológica e Recursos Naturais, Universidade Regional do Cariri, Rua Cel. Antônio Luiz, 1161, 63.105-000, Crato CE, Brazil*
[10]*Departamento de Biologia, Instituto de Ciências Biológicas, Universidade Federal do Amazonas, 69080-900, Manaus, AM, Brazil*
[11]*Department of Ecology and Vertebrate Zoology, Faculty of Biology and Environmental Protection, University of Łódź, 12 / 16 Banacha Str., Łódź 90-237, Poland*
[12]*Departamento de Genética, Instituto de Ciências Biológicas, Universidade Federal do Amazonas, 69080-900, Manaus, AM, Brazil*
[13]*Department of Biological Sciences, Universidad de los Andes, Bogotá, 111711, Colombia*
[14]*Museo de Zoología, Escuela de Biología, Pontificia Universidad Católica del Ecuador, Quito, Ecuador*
[15]*Corporación para el Desarrollo Sostenible del Sur de la Amazonia-CORPOAMAZONIA, Mocoa, Putumayo, Colombia*

*Corresponding author. E-mail: fouquet.antoine@gmail.com

[16]*Ecosfera Consultoria e Pesquisa em Meio Ambiente LTDA. Rodovia BR-259 s/n, Fazenda Bela Vista, Itapina, ES, Brazil*
[17]*Departamento de Zoologia, Universidade Federal de Pernambuco, Av. Professor Moraes Rego, S/N, Cidade Universitária, 50760-420, Recife, PE, Brazil*
[18]*Museum of Zoology, Senckenberg Natural History Collections Dresden, Dresden, Germany*
[19]*The Natural History Museum, Cromwell Road, London SW7 5BD, UK*
[20]*Palaeontological Institute and Museum, University of Zurich, Zurich, Switzerland*

Received 2 October 2020; revised 9 November 2020; accepted for publication 9 November 2020

The outstanding biodiversity of the Guiana Shield has raised many questions about its origins and evolution. Frogs of the genera *Adelastes*, *Otophryne* and *Synapturanus* form an ancient lineage distributed mostly across this region. These genera display strikingly disparate morphologies and life-history traits. Notably, *Synapturanus* is conspicuously adapted to fossoriality and is the only genus within this group to have dispersed further into Amazonia. Moreover, morphological differences among *Synapturanus* species suggest different degrees of fossoriality that might be linked to their biogeographical history. Through integrative analysis of genetic, morphometric and acoustic data, we delimited 25 species in this clade, representing a fourfold increase. We found that the entire clade started to diversify ~55 Mya and *Synapturanus* ~30 Mya. Members of this genus probably dispersed three times out of the Guiana Shield both before and after the Pebas system, a wetland ecosystem occupying most of Western Amazonia during the Miocene. Using a three-dimensional osteological dataset, we characterized a high morphological disparity across the three genera. Within *Synapturanus*, we further characterized distinct phenotypes that emerged concomitantly with dispersals during the Miocene and possibly represent adaptations to different habitats, such as soils with different physical properties.

ADDITIONAL KEYWORDS: Amazonia – Amphibia – integrative taxonomy – micro-computed tomography – mitogenomics.

INTRODUCTION

The Neotropics harbour the most diverse terrestrial ecosystems on the planet (Jenkins *et al.*, 2013). Within them, Amazonia has a paramount role both in terms of geographical extent (> 6.5×10^6 km^2; 40% of the world's tropical rainforests) and biodiversity (Myers *et al.*, 2000; Antonelli *et al.*, 2018). The Guiana Shield occupies the northern part of Amazonia and is defined by a Precambrian geological formation once connected to Africa (Hammond, 2005). This region is mostly covered by lowland Amazonian forest and savannas, but also features peculiar, high-elevation sandstone mountains (tepuis) hosting ancient lineages of isolated relict species (e.g. Kok *et al.*, 2012, 2018; Kok, 2013; Rull & Vegas-Vilarrúbia, 2020). Despite the astounding diversity of the Guiana Shield, our understanding of the number and distribution of species remains largely incomplete (Vacher *et al.*, 2020). Consequently, the historical causes and regional determinants of this outstanding diversity are still largely speculative (Kok, 2013; Rull & Vegas-Vilarrúbia, 2020).

Several anuran clades occurring in the Guiana Shield have repeatedly been documented to contain many unnamed species, whose distribution patterns could provide crucial insights into the past of Amazonia (Kok *et al.*, 2017; Vacher *et al.*, 2017; Réjaud *et al.*, 2020). Two major groups make up the majority of Neotropical anurans, Hyloidea and Microhylidae (81 and 18% of Neotropical species, respectively), which diversified dramatically from the end of the Cretaceous and early Palaeogene onwards (Feng *et al.*, 2017). Microhylidae currently includes 702 valid nominal species (Frost, 2020), and its history was highly influenced by the break-up of Gondwana. Since then, each of its major lineages has diversified independently on the different continental masses (Asia, Africa, Pacific and America) (Tu *et al.*, 2018; Streicher *et al.*, 2020). Extant Neotropical microhylids belong to two major groups: Gastrophryninae, the most species-rich subfamily, with 79 species (Frost, 2020) distributed from southern North America to Argentina; and a species-poor clade formed by Adelastinae and Otophryninae (Peloso *et al.*, 2016; Hime *et al.*, 2021), which contains only seven species (one *Adelastes*, three *Otophryne* and three *Synapturanus*), all originally described from the Guiana Shield.

Adelastes, *Synapturanus* and *Otophryne* are so distinct in their morphology and ecology that they have not been considered as being closely related (see Zweifel, 1986; Wild, 1995) until genetic data were used in phylogenetic studies (Pyron & Wiens, 2011; Trueb *et al.*, 2011; de Sá *et al.*, 2012; Peloso *et al.*, 2016; Tu

et al., 2018; Hime *et al.*, 2021). *Otophryne* have a semi-fossorial lifestyle and forage in the leaf litter, which they mimic through the leaf-like shape of their bodies and coloration (Campbell & Clarke, 1998). In addition, they are diurnal, territorial and associated with streams, in which their exotrophic tadpoles develop (Wassersug & Pyburn, 1987; MacCulloch *et al.*, 2008). One species is found in the lowlands (*Otophryne pyburni* Campbell & Clarke, 1998), one at mid-elevations (*Otophryne robusta* Boulenger, 1900) and one even inhabits the summits of tepuis of the Chimantá Massif, ≤ 2168 m a.s.l. (*Otophryne steyermarki* Rivero, 1968). All known *Synapturanus* species occur in the lowlands and are markedly adapted to fossoriality. Owing to their fossorial habits and their very brief reproductive period (Nelson & Lescure, 1975; Ernst *et al.*, 2005), their life histories are poorly documented. Individuals have been observed in underground galleries and nuptial chambers, which they dig to deposit eggs that undergo endotrophic development (Nelson & Lescure, 1975; Pyburn, 1975, 1977; Menin *et al.*, 2007). Although no direct observations have been reported, the overall morphology and, notably, the shape of the humerus of *Synapturanus mirandaribeiroi* Nelson & Lescure, 1975, suggest forward-burrowing behaviour (Keeffe & Blackburn, 2020). In addition, these are crepuscular and nocturnal frogs, associated with well-drained soils of *terra-firme* (non-flooded) forests. The ecology of the monotypic *Adelastes* is even less documented. These frogs are found in the lowlands and are apparently semi-fossorial and associated with temporary ponds (Zweifel, 1986; Almeida *et al.*, 2014).

Species boundaries, distributions and the evolutionary history of these three genera are also extremely poorly known. Consequently, there is a limited amount of material available in collections, and phylogenetic studies including these groups are largely lacking, perhaps apart from studies addressing intergeneric relationships (Pyron & Wiens, 2011; de Sá *et al.*, 2012; Peloso *et al.*, 2016; Tu *et al.*, 2018; Hime *et al.*, 2021; Streicher *et al.*, 2021). Given these multiple shortfalls in knowledge, it is challenging to formulate testable hypotheses with respect to the biogeographical and phenotypic diversification of this peculiar group of frogs. However, diversification from within the Guiana Shield and subsequent dispersal into the wider Amazonian region seems likely when considering the present distribution of the group. Moreover, large water bodies, such as major rivers and the Pebas system, a lacustrine environment that occupyied most of Western Amazonia from the early Miocene 23 Mya until 10–9 Mya (Hoorn *et al.*, 2010, 2017), probably imposed barriers to dispersal and gene flow for these species associated with *terra-firme* forest. Therefore, the dispersal and diversification of *Synapturanus* throughout Amazonia might have been influenced by the successive hydrological transformations of Amazonia during the last 23 Mya.

Although these genera are understudied, a few observations on the morphological variation among and within them have been made. Osteological diversity in microhylids probably exceeds that of any other anuran family, and this diversity is especially evident in New World taxa (Trueb *et al.*, 2011). The large osteological variation seen within Microhylidae is likely to be linked to their repeated evolution towards fossoriality (Wild, 1995). Moreover, morphological disparity also exists within *Synapturanus*, potentially attributable to differences in fossorial habits. *Synapturanus rabus* Pyburn, 1977 is smaller and has a more slender body and relatively larger eyes than *S. mirandaribeiroi* and *Synapturanus salseri* Pyburn 1975, which led Pyburn (1977) to suggest that *S. rabus* might be less fossorial. Morphological modifications of the skull (hyperossification) and robust forelimbs have been considered adaptations to fossoriality (Emerson, 1976; Nomura *et al.*, 2009; Vidal-García & Keogh, 2017; Keeffe & Blackburn, 2020; Paluh *et al.*, 2020). Considering the varied life-history traits and morphologies seen in these three genera, skull and forelimb traits might have evolved differently among and within them, particularly in fossorial species.

To address our overarching question of how historical environmental changes might have driven speciation and phenotypic diversification in the understudied frog genera *Synapturanus*, *Otophryne* and *Adelastes*, we analysed genetic, morphometric, acoustic and three-dimensional (3D) osteological data in an integrative approach. More specifically, we: (1) delimited the extant species; (2) inferred their phylogenetic relationships and investigated their historical biogeography, focusing on their spatial origin and the timing of diversification within the Guiana Shield and Western Amazonia; and (3) evaluated the link between diversification and anatomical evolution in relationship to fossoriality. By overcoming the challenging task of assembling diverse types of data over the range of this group of frogs, our integrative approach represents a leap forwards in our understanding of their biology and evolutionary history.

MATERIAL AND METHODS

Species delimitation

DNA-based delimitation

Our first objective was to delimit major mitochondrial DNA (mtDNA) lineages within the three focal genera. Our sampling included a fragment of 16S rDNA sequences from 90 specimens of *Adelastes*, *Otophryne* and *Synapturanus* (Supporting Information, Table

S1) and covered the entire range of the three genera. These samples were obtained through fieldwork and loans and were completed with available sequences from GenBank (Supporting Information, Table S1). Newly generated sequences were obtained from Sanger sequencing (details of primers are available in Supporting Information, Table S2; further technical details are given in Supporting Information, Appendix S1). DNA sequences were aligned on the MAFFT online server under the E-INS-i option with default parameters (Katoh *et al.*, 2017).

We applied three DNA-based single-locus species delimitation approaches using this dataset: (1) a distance-based method, the automated barcode gap discovery (ABGD; Puillandre *et al.*, 2012); (2) a multi-rate coalescent-based method, the multi-rate Poisson tree processes model approach (mPTP; Kapli *et al.*, 2017); and (3) a single-threshold coalescent-based method, the generalized mixed Yule coalescent approach (single-threshold GMYC; Pons *et al.*, 2006; Monaghan *et al.*, 2009). The ABGD delimitation was performed using the online Web server (available at: https://bioinfo.mnhn.fr/abi/public/abgd/abgdweb.html) with a prior of intraspecific divergences (JC69) between 0.001 and 0.1 (P = 0.001–0.1), a proxy for minimum relative gap width of one (X = 1) and a number of steps equals to 30 (N = 30). For the mPTP delimitation, we first reconstructed a maximum likelihood (ML) tree with RAxML v.8.2.4 (Stamatakis, 2014) using a GTR+I+Γ model, which was estimated to be a suitable model via PartitionFinder v.2.1.1 (Lanfear *et al.*, 2017). The mPTP delimitation was undertaken on the tree rooted on *Adelastes*, with 5×10^6 Markov chain Monte Carlo (MCMC) iterations, sampling every 10 000th iteration and discarding the initial 10% of iterations as burn-in. For the GMYC delimitation, we reconstructed a time-calibrated phylogeny using BEAST 2.5 (Bouckaert *et al.*, 2014). We used a birth–death population model to account for extinction processes and incomplete sampling. We used a single partition with a GTR+I+Γ substitution model, with an uncorrelated relaxed lognormal clock model of rate variation among branches (Drummond *et al.*, 2006). We used the estimated age of the most recent common ancestor (MRCA) of the three genera by Feng *et al.* (2017) as a calibration point, assuming a normal prior distribution of 59.6 Mya (SD = 3.6 Mya). For the MCMC parameters, we used four independent chains of 1×10^8 iterations, recording every 10 000th iteration and discarding the first 10% of iterations as burn-in. We combined the log files of the four independent runs using LogCombiner v.2.5 (Bouckaert *et al.*, 2014) and checked the appropriate mixing of our model parameters, using a threshold of effective sample size > 200. Then, we calculated the maximum clade credibility tree (from 3604 trees) using TreeAnnotator v.2.5 (Bouckaert *et al.*, 2014). We performed a GMYC delimitation on the ultrametric tree using the GMYC function of the SPLITS package in R v.3.2.4 (Ezard *et al.*, 2009), with the single-threshold method set at an interval between 0 and 10 Mya. Operational taxonomic units (OTUs) were defined using a majority-rule consensus from the results of the three methods, i.e. a lineage is considered an OTU if supported by at least two of the three methods.

External morphology within Synapturanus

In order to investigate patterns of morphological variation within *Synapturanus* (phenotypic differentiation within *Otophryne* and *Adelastes* was not examined because insufficient data were available), in addition to congruence between morphological differences and DNA-based delimitation, we examined 65 specimens deposited in various zoological collections (Supporting Information, Tables S1 and S3). Among those specimens, 29 were included in the molecular dataset and, thus, directly linked to DNA-based OTUs. The other 36 specimens were assigned to one of the OTUs defined here (see above) based on morphological examination and on the geographical proximity of their collecting locality relative to that of a genotyped specimen. Examined specimens represented 25 sampling sites and belonged to 15 OTUs, including a paratopotype of *S. mirandaribeiroi*.

We measured 12 morphological variables on examined specimens, following Kok & Kalamandeen (2008): snout–vent length (SVL); head length, from the corner of the mouth to the tip of the snout (HL); head width at the level of the angle of jaws (HW); eye-to-naris distance, from the anterior edge of the eye to the centre of the naris (EN); internarial distance (IN); horizontal eye diameter (ED); interorbital distance, representing the width of the underlying frontoparietals (IO); forearm length, from the proximal edge of the palmar tubercle to the outer edge of the flexed elbow (FAL); hand length, from the proximal edge of the palmar tubercle to the tip of finger III (HAND); crus (tibiofibular) length, from the outer edge of the flexed knee to the heel (TL); foot length, from the proximal edge of the inner metatarsal tubercle to the tip of the toe IV (FL); and thigh length, from the vent opening to the outer edge of the flexed knee (ThL). We examined variation in morphometric data through a principal components analysis (PCA) via the FactoMineR package in R v.3.2.4 (Lê *et al.*, 2008; R Core Team, 2016). To control for variation in body size among individuals, we also performed additional analyses on a size-corrected dataset (residuals) obtained by linear regression of the original morphometric measures of each variable on SVL (Strauss, 1985). We considered that an absence of overlap among OTUs along the different PCA axes

using size-corrected and uncorrected data confirmed their delimitation as distinct putative species.

Bioacoustics within Synapturanus

We investigated patterns of acoustic variation and its congruence with DNA-based OTUs. We gathered call recordings of 44 males of *Synapturanus* from various sources (Supporting Information, Table S4), including the calls of *S. rabus* and *S. salseri* from their type localities, totalling 19 sampled sites and 14 OTUs (see Results; new recordings have been deposited at sonotheque.mnhn.fr). We measured three call variables following those standardized by Köhler *et al.* (2017): note length (NL); dominant frequency (DoF; taken with a spectral slice over the entire note); and delta frequency (DeF; the difference in peak frequency between spectral slices taken over the first and the last 0.015 s of the note). The temporal and spectral variables were measured from waveforms and spectrograms of one note per recorded male, respectively, using AUDACITY v.2.4.1 (Audacity Team, 2020). These recordings are heterogeneous in terms of length and quality. Information on recording equipment, distance from source and air temperature during the recording were not available in most cases. Notes recorded with high quality were often single or in very low numbers per record, and we chose the ones with the best quality to measure acoustic variables. When more than one call was available per recorded male, these variables varied little. All *Synapturanus* species emit single-note calls, with a highly variable intraspecific rate of emission, apparently depending on activity. Therefore, we did not measure silent intervals between calls. Owing to their fossorial ecology, recorded specimens were rarely collected and thus, often could not be assigned directly to genotyped specimens. Nevertheless, with one exception, these identifications were not ambiguous, because single species were collected at the localities of the recordings or because calls were readily differentiated when two species co-occurred (i.e. near Manaus, Amazonas, Brazil). We examined acoustic variation through a PCA (function PCA, on the correlation matrix) via FACTOMINER in R v.3.2.4. Two species (*Synapturanus* sp. 'Manaus' and *Synapturanus* cf. *mirandaribeiroi*) were not included in the PCA because they emit pulsed notes, whereas the other species emit tonal notes. We considered that an absence of overlap among related OTUs along the different PCA axes confirmed the genetic delimitation.

Integrative species delimitation within Synapturanus

In order to reach a diagnostic species delimitation, i.e. to classify each candidate species (CS) as a confirmed candidate species (CCS), an unconfirmed candidate species (UCS) or a deep conspecific lineage (DCL), we followed the framework of Vieites *et al.* (2009). We considered as 'confirmed' any CS for which there was at least one congruent difference in any character other than the primary molecular divergence criterion between close relatives. We considered as 'unconfirmed' any CS for which additional evidence was lacking. Nonetheless, phenotypically similar OTUs that were not sister to each other were also considered CCS (Castroviejo-Fisher *et al.*, 2017).

Taxonomy and distribution

We assigned these OTUs to available taxa after examining type material and considering original descriptions, spatial origin, morphology and acoustic data. We present the evidence used to associate OTUs with taxon names below.

Otophryne pyburni was described from the lowlands of the western part of the Guiana Shield (Colombia, Vaupés). Lowland populations from French Guiana and the Brazilian state of Amapá (2000 km east of Vaupés) were previously assigned to *O. robusta* but tentatively transferred to *O. pyburni* (Campbell & Clarke, 1998). Other populations of *Otophryne* from the Pantepui region have been tentatively assigned to this taxon (Carvalho *et al.*, 2007), and disjunct populations of the highland species *O. steyermarki* on different tepuis might conceal cryptic diversity (Kok *et al.*, 2017, 2018). DNA sequences of *O. steyermarki* from the type locality allow assignation of an OTU to this taxon (see Results). One partial mitogenomic sequence from the type locality of *O. pyburni* was available, although lacking 16S, and was therefore not included in the DNA-based species delimitation. However, these data allow assignation of an OTU to this taxon in subsequent analyses. *Otophryne robusta* is described from the foot of Mt Roraima. DNA sequences from specimens collected near to this locality unambiguously correspond to this taxon.

Adelastes hylonomos Zweifel, 1986 was described from southern Venezuela, but has been collected more recently in nearby Brazil (Almeida *et al.*, 2014) and from an additional locality in Guyana (Peloso *et al.*, 2016). Its phylogenetic position was investigated exclusively based on DNA sequences obtained from the Guyanan population, 1000 km away from the type locality (Peloso *et al.*, 2016). Material collected close to the type locality, in Brazil, allows assignation of an OTU to this taxon.

All three previously named species of *Synapturanus* have ambiguous records, and none of the available DNA sequences can be assigned undoubtedly to nominal species. *Synapturanus mirandaribeiroi* was described based on specimens from Kanashen

(also spelled 'Konashen', Southern Guyana) and was reported throughout the Guiana Shield (Nelson & Lescure, 1975; Lima *et al.*, 2006; Menin *et al.*, 2007; Barrio-Amorós *et al.*, 2019), including the right bank of Negro River, in the Jaú National Park (Neckel-Oliveira & Gordo, 2004). However, Motta *et al.* (2018) and Fouquet *et al.* (2019) suspected that there are several species under this epithet in the Eastern Guiana Shield, whereas Vacher *et al.* (2020) hypothesized that at least four different species exist in this region. DNA sequences from populations surrounding the type locality are available, but ambiguity remains despite morphological examination of the type specimen (see Results). We tentatively assigned the name *S. mirandaribeiroi* to sampled populations distributed in Suriname, Southern French Guiana and Northern Amazonas state, Brazil, considering distribution and morphology. *Synapturanus rabus* was described based on samples from Vaupés, Colombia (Western Guiana Shield), but populations from Ecuador (Read, 2000; Ortiz, 2018) and Peru (Gordo *et al.*, 2006; López-Rojas & Cisneros-Heredia, 2012; Gagliardi-Urrutia *et al.*, 2015) have been assigned tentatively to this taxon. DNA sequences from a population located 150 km south of the type locality were assigned tentatively to this taxon. *Synapturanus salseri* was also described from Vaupés, Colombia, and populations from Manaus region of Brazil (Lima *et al.*, 2006; Menin *et al.*, 2007), Venezuela (Barrio-Amorós *et al.*, 2019) and Guyana (Kok & Kalamandeen, 2008) have also been assigned tentatively to this taxon. Unfortunately, no DNA sequences assignable to this taxon were available. However, a call recording from the type locality of *S. salseri*, in addition to a paratype, were included in subsequent morphological analyses.

Divergence time estimates

We selected one representative for each delimited OTU (N = 25 plus one additional *Otophryne*; see Results) for inference of phylogenetic relationships and estimation of divergence times. We obtained whole mitogenomic data for 19 samples (representatives of the major lineages) via shotgun sequencing and one available mitogenome from GenBank (Supporting Information, Table S1; methodological details are available in Supporting Information, Appendix S1). We completed the mtDNA matrix for the remaining seven terminals for the following loci: 12S, 16S, *COI* and *Cytb* via Sanger sequencing, complemented with available GenBank sequences (Supporting Information, Table S1), and three nuclear DNA (nuDNA) loci (*POMC*, *RAG1* and *TYR*; Supporting Information, Table S1), again obtained via Sanger sequencing (for details of primers, see Supporting Information, Table S2). During the matrix building, we identified two sequences in GenBank that appear to be misidentified (*Kaloula POMC*, GenBank accession HM998968, and *Adelastes TYR*, GenBank accession KM509882), which were thus discarded. Additionally, we retrieved mitogenomes and homologous nuDNA sequences for ten outgroups representing major microhylid lineages and one ranid species from the GenBank database. DNA sequences were realigned on the MAFFT online server under the E-INS-i option for 12S and 16S and under the G-INS-i option for coding sequences, with default parameters (Katoh *et al.*, 2017). Codon insertion–deletions were checked and realigned according to the reading frame. The final alignments had lengths of 15 744 bp for mtDNA and 2528 bp for concatenated nuDNA. Three OTUs had > 4500 bp available, and three OTUs were represented by only 550 bp of the 16S gene. For six OTUs, nuDNA data were not available for the sample with the most complete mtDNA data (list in Supporting Information, Table S5). We therefore reduced the amount of missing data per terminal and reduced computing time during phylogenetic analyses by assigning sequences from different conspecific specimens from the same or nearby populations (confirmed by mtDNA) to a single composite terminal (Wilkinson, 1995; Kearney, 2002; Campbell & Lapointe, 2009). We performed a preliminary maximum likelihood analysis of the nuDNA using RAxML (see DNA-based delimitation section) performed to test overall congruence with mtDNA (Supporting Information, Fig. S1).

We selected the best-fitting partition scheme and model of evolution for each partition using PartitionFinder v.2.1.1 (Lanfear *et al.*, 2017), according to the Bayesian information criterion (BIC). We predefined eight blocks, one for ribosomal RNA genes (12S and 16S), one for transfer RNA genes, one for each codon position of concatenated mtDNA CDS regions, and one for each codon position of concatenated nuDNA CDS regions.

We reconstructed a time-calibrated gene tree in BEAST 2.5 using a birth–death tree prior to account for extinction processes. We parameterized unlinked substitution models according to the models suggested by the PartitionFinder analysis. Divergence time estimation was implemented using an uncorrelated relaxed log-normal clock model of the distribution of rates among branches for each partition (Drummond *et al.*, 2006). Owing to the absence of Otophryninae fossils, we relied on secondary calibration points (including SD) based on the study by Feng *et al.* (2017), an extensive nuclear genomic dataset (88 kb) of all major frog lineages. Specifically, we assumed a normal prior distribution to calibrate the following five nodes: (1) the MRCA of Microhylidae and Ranidae (mean = 100.9 Mya, SD = 4.9 Mya), which corresponds to the root

of the tree; (2) the crown age of Microhylidae (mean = 67.1 Mya, SD = 3.7 Mya); (3) the crown age of Gastrophryninae (mean = 48.1 Mya, SD = 3.5 Mya); (4) the MRCA age of Microhylinae + Asterophryinae (mean = 54.8 Mya, SD = 3.4 Mya); and (5) the MRCA of Gastrophryninae and Otophryninae + *Adelastes* (mean = 59.6 Mya, SD = 3.6 Mya). We enforced the monophyly of Gastrophryninae and of Microhylidae because these clades have been strongly supported in recent phylogenomic analyses (Feng *et al.*, 2017; Hime *et al.*, 2021). We set four independent MCMC runs of 1×10^8 iterations each, recording every 10 000th iteration and using the first 10% of iterations as burn-in. We combined the log files and the resulting posterior samples of trees of the four independent runs using LogCombiner v.2.5 (Bouckaert *et al.*, 2014) and checked convergence of model parameters via time-series plots. Chain mixing was considered adequate when parameters achieved an effective sample size > 200 (obtained for all parameters). We calculated a maximum clade credibility tree (based on the 36 004 resulting trees) using TreeAnnotator v.2.5 (Bouckaert *et al.*, 2014).

Biogeographical analyses

We used the resulting time-calibrated phylogeny to infer ancestral areas and biogeographical events in the BioGeoBEARS package in R (Matzke, 2013). We compared three models: (1) a likelihood version of the dispersal–vicariance model (DIVALIKE; Ronquist, 1997); (2) a likelihood version of the BayArea (BBM) model (Landis *et al.*, 2013); and (3) the dispersal–extinction–cladogenesis model (DEC; Ree & Smith, 2008). We also compared versions of these models allowing jump-dispersal as described by the J parameter (Matzke, 2013; Ree & Sanmartín, 2018; Klaus & Matzke, 2020). Models were compared using the Akaike information criterion (AIC). To determine biogeographical event counts for the best-fitting model, we ran the BioGeoBEARS biogeographical stochastic mapping 50 times (Dupin *et al.*, 2017). To identify spatial processes of diversification, we considered four main geographical areas where known species currently occur: Western Guiana Shield (WG), Eastern Guiana Shield (GU), Western Amazonia (WA) and Brazilian Shield (BS). They correspond to major geological features of Amazonia (Hoorn *et al.*, 2010) and to the large biogeographical regions known as Wallace's districts (Wallace, 1854), roughly delimited by modern riverine barriers: the Madeira River, the Caqueta/Japurá–Solimões and the lower course of the Amazon River. The Guiana Shield is further bisected into two main areas, Western and Eastern, which correspond to two main blocks separated by the Rupununi–Essequibo depression. This depression separates Pantepui in the West from the hilly but low-lying landscape of the eastern part of the Guiana Shield, which has been shown to harbour distinct anuran communities (Vacher *et al.*, 2020). This spatial partitioning into four areas allows us to investigate the possible influence of the Pebas system during the early Neogene and possible dispersals between the Eastern and Western Guiana Shield, and across the Amazon River, over the last 10 Myr (Vacher *et al.*, 2017; Réjaud *et al.*, 2020).

Shape analysis

To investigate patterns of morphological variation in relationship to phylogeny and the historical biogeography across the entire focal clade (i.e. *Adelastes*, *Otophryne* and *Synapturanus*), we gathered morphometric data from micro-computed tomography scans of 49 specimens selected to represent as many OTUs as possible (21 OTUs; Supporting Information, Table S6). Specimens were scanned (at 40–70 kV, resolution < 20 µm) using an EasyTom 150 from the magnetic resonance imaging platform of the Institute of Evolutionary Sciences of Montpellier (ISEM), a GE phoenix v|tome|x s240 (American Museum of Natural History), a Bruker Skyscan 1173 (Pontifícia Universidade Católica do Rio Grande do Sul) or a Bruker Skyscan 1176 (Universidade de São Paulo). We obtained scans of 30 *Synapturanus* specimens, representing 13 OTUs (out of 17 OTUs + *S. salseri* and *S. mirandaribeiroi* paratopotypes); six *Otophryne* specimens, representing five (out of seven) OTUs (including *O. pyburni* paratopotype); and four *Adelastes* specimens, representing both OTUs (including *A. hylonomos* holotype) (data of the scans are deposited at http://morphosource.org/; Supporting Information, Table S6). Twenty-five specimens used in this shape analysis were also genotyped and could thus be linked directly to the DNA-based species delimitation. The remaining nine micro-computed tomography-scanned specimens were unambiguously assigned to OTUs because they were from the same populations as genotyped specimens where no co-occurring species have been sampled. In order to compare and contrast the morphological variation of our samples to those of different species of Gastrophryninae (*Chiasmocleis*, *Elachistocleis*, *Arcovomer*, *Gastrophryne* and *Myersiella*) and other microhylids (*Barigenys* and *Xenorhina*) that evolved various degrees of specialization to fossoriality independently (Supporting Information, Table S7), we included nine additional scans, of which two were obtained from MorphoSource (www.morphosource.org) (Supporting Information, Table S6).

We focused on the cranium and the humerus because both structures are considered to represent

good proxies for adaptation to fossoriality in frogs (Emerson, 1976; Vidal-García & Keogh, 2017; Paluh *et al.*, 2020). Segmentation of the cranium and the humerus was done using AVIZO (FEI Visualization Sciences Group, Burlington, MA, USA). All the mesh files were subsequently imported as PLY files into GEOMAGIC WRAP (3D Systems, Rock Hill, SC, USA) in order to clean, repair and decimate the meshes before the landmarking procedure. To depict the shape of the cranium and the humerus accurately, we used a geometric morphometric approach and acquired 142 landmarks on the skull and eight landmarks on the humerus (Supporting Information, Fig. S2) using IDAV LANDMARK (http://graphics.idav.ucdavis.edu/research/EvoMorph). Procrustes superimpositions (Rohlf & Slice, 1990) were done for the cranium using the 'bilat.symmetry' function from the geomorph R package (Adams *et al.*, 2019). When two or more specimens were available, a single mean shape was calculated for each species using the Procrustes coordinates.

Principal components analyses were performed independently for both anatomical structures using the mean shape of each species to investigate the distribution of OTUs in the morphological space (morphospace) and to investigate the putative link with fossorial lifestyle. To do so, the 'plotTangentSpace' function of the geomorph R package (Adams *et al.*, 2019) was used. We subsequently mapped the phylogeny onto the morphospace using the function 'phylomorphospace' from the phytools R package (Revell, 2012). Given that the phylogenetic positions of *S. salseri* and *S. mirandaribeiroi* remain elusive in the absence of molecular data from topotypical material, we tentatively assigned *S. salseri* as sister to the other species of the Eastern clade and *S. mirandaribeiroi* as sister to *Synapturanus* cf. *mirandaribeiroi* (see Results).

Covariation between cranial and humeral shapes was investigated using a two-block partial least squares (2B-PLS) analysis and the function 'pls2B' from the Morpho R package (Schlager, 2013). This analysis was carried out first on the same microhylid family-level dataset and then again on *Synapturanus* only, in order to provide details on shape variation within the genus. Given that species share evolutionary history, they cannot be treated as independent data points; thus, we tested further for covariation using the 'phylo.integration' function from the geomorph R package (Adams *et al.*, 2019). Shape changes along principal component (PC) axes were visualized using thin-plate-spline deformation and the vector displacement of landmarks using the functions 'plsEffects', 'warp.mesh', 'plotRefToTarget' and 'shade3d' from the Morpho (Schlager, 2013) and rgl (Adler & Murdoch, 2012) R packages.

RESULTS

SPECIES DELIMITATION

The phylogenetic trees obtained from the ML and the Bayesian analyses of 577 bp of the 16S locus strongly support the three focal genera and three major clades within *Synapturanus* as monophyletic. These major Synapturanus clades are restricted to Western, Central and Eastern Amazonia and dubbed accordingly (Fig. 1A). Several deeply diverging lineages are supported within the three focal genera, indicating a vast underestimation of the species diversity in this clade (Fig. 1A; Supporting Information, Fig. S3).

Of the three species delimitation methods, ABGD was found to be the most conservative, delimiting 21 OTUs. We kept the 12th–17th partitions (P = 0.0057–0.0127) based on two criteria: (1) they correspond to a plateau for group number; and (2) this is close to the 1% arbitrary threshold of intraspecific divergence recognized in other vertebrate delimitation studies using the 16S locus (Puillandre *et al.*, 2012) (Supporting Information, Table S11). In contrast, mPTP and GMYC delimited 23 and 27 OTUs, respectively (Fig. 1A). The mean interspecific pairwise distance (p-distance) among these OTUs reaches a minimum value of 1.7% and is < 3% in six instances (Supporting Information, Table S8). The consensus of the results obtained through the three methods led to the delimitation of 23 DNA-based OTUs (15 *Synapturanus*, six *Otophryne* and two *Adelastes*; Fig. 1A). In the case of *Synapturanus* sp. 'Purus', *Synapturanus* sp. 'Taboca' and *Synapturanus* sp. 'Tapajós', the three methods led to discordant results. Considering their respective distributions within distinct interfluvia, notably across the Amazon River, their distinct calls and morphology (although uncertain owing to the low number of available specimens; see below and Supporting Information, Appendix S2) we considered them as different OTUs (as suggested by the GMYC results), for a total of 25 OTUs.

The first two components of the PCA based on raw morphometric measurements accounted for 89.5% of the total variation (Fig. 1B; Supporting Information, Table S9). Overall, the variation along the first PC axis is related to body size and illustrates that western and central Amazonian species are smaller than eastern species. The variation in body size among the eastern species is also substantial, with a subgroup formed by the easternmost species being larger than the early-diverging *Synapturanus* sp. 'Guyana' and

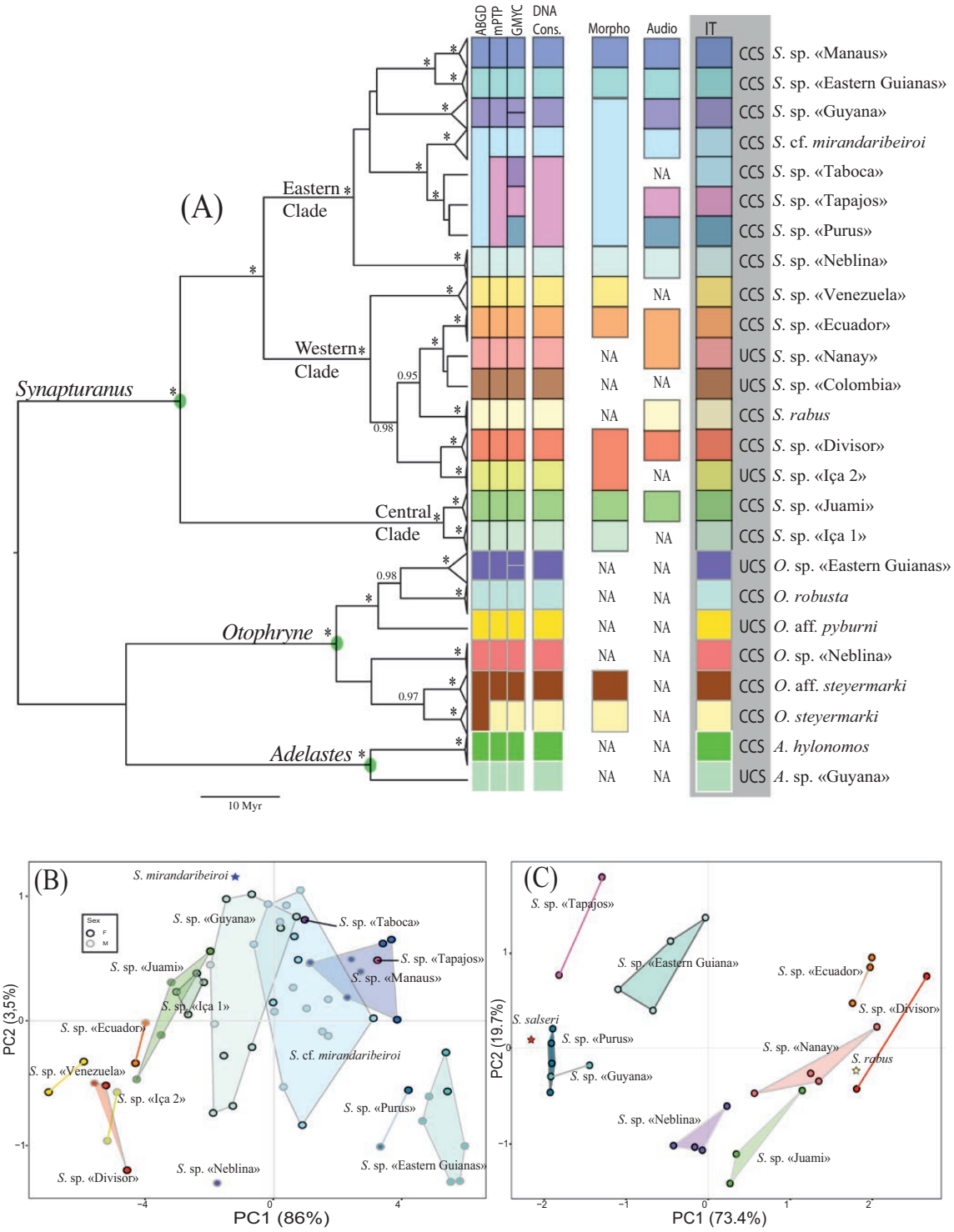

Figure 1. Phylogenetic relationships (A), morphological (B) and acoustic (C) variation and species delimitation of Otophryninae (red node) + *Adelastes*. A, majority rule consensus tree inferred by Bayesian analysis with BEAST 2 using 577 bp of 16S ribosomal DNA of the target genera *Adelastes*, *Otophryne* and *Synapturanus* (green nodes). Asterisks indicate node posterior probabilities > 0.95; lower values are not indicated. Some terminal branches are collapsed according to the results of the DNA-based species delimitation (ABGD, mPTP and GMYC) (complete tree is given in Supporting Information, Fig. S2). Congruence with variation in external morphology (Morpho) and bioacoustics (Audio), in addition to the integrative

Synapturanus sp. 'Neblina'. Variation along PC2 and with size corrected data is notably related to eye diameter (Supporting Information, Fig. S4).

Morphological analyses (Fig. 1B) suggested many non-overlapping OTUs in morphospace despite close phylogenetic relatedness. This is the case in *Synapturanus* sp. 'Eastern Guianas' vs. *Synapturanus* sp. 'Manaus', which is consistent with the results of the DNA-based delimitation. *Synapturanus* sp. 'Juami' and *Synapturanus* sp. 'Içá 1' do not overlap when comparing PC2 vs. PC3 or considering size-corrected measurements (Supporting Information, Fig. S4; Appendix S2), confirming primary delimitation. In contrast, *Synapturanus* sp. 'Içá 2' and *Synapturanus* sp. 'Divisor' overlap along all examined axes. The morphological distinction between *Synapturanus* sp. 'Taboca' and *S.* cf. *mirandaribeiroi* remains uncertain (Supporting Information, Appendix S2). It is noteworthy that the type specimen of *S. mirandaribeiroi* is not embedded within the morphospace of any OTU in either uncorrected or size-corrected analyses. Nevertheless, this specimen is comparatively similar to *Synapturanus* sp. 'Taboca' and *S.* cf. *mirandaribeiroi*, both of which are geographically close to the type locality of *S. mirandaribeiroi*.

Acoustic data, in contrast, appeared to be more powerful in discriminating OTUs within *Synapturanus*, with mostly non-overlapping clusters of DNA-based OTUs in the multidimensional acoustic space. The two first components accounted for 93.1% of the total variation in call parameters (Fig. 1C; Supporting Information, Table S10). The species of the Western clade (Fig. 2) emit short (NL < 0.1 s) and high-pitched (DoF > 1.6 kHz) tonal notes and cluster together in the multidimensional space. Within the Central clade, only the call of *Synapturanus* sp. 'Juami' was available, thus preventing us from evaluating call variation. Within the Eastern clade, there is a pronounced call variation and no overlap between the eight DNA-based OTUs (Fig. 1C). The other species of the Eastern clade vary greatly in NL and DoF. The call of *S. salseri* clearly clustered with other Eastern clade species, which is consistent with patterns of anatomical similarity (see shape analysis; Supporting Information, Table S10).

The combination of external morphology and bioacoustics supports the specific status of 16 out of 25 OTUs identified by DNA-based delimitation analyses (12 CCS in *Synapturanus*, three in *Otophryne* and one in *Adelastes*). Additionally, considering the relationships among OTUs, three additional OTUs can be confirmed. Finally, six OTUs remain unconfirmed (three UCS in *Synapturanus*, two in *Otophryne* and one in *Adelastes*; Fig. 1A; Supporting Information, Table S11). A detailed justification for confirmed and unconfirmed status is provided in the Supporting Information (Appendix S2).

Divergence times and biogeography

Following the results of the PartitionFinder analysis, we assigned substitution models to each of the eight partitions defined a priori. The best-fitting model for all partitions was GTR+I+Γ, except for the first codon position of the nuDNA dataset (TRN+Γ). The four combined BEAST runs led to all parameters having an effective sample size > 500. The resulting phylogenetic relationships within the maximum clade credibility tree were strongly supported (posterior probability (pp > 0.98), with two exceptions involving shallow divergences within *Synapturanus* clades among terminals represented only by 16S (Fig. 3). The previously recovered three major clades (Western, Central and Eastern Amazonia) were also identified within *Synapturanus*. *Adelastes* is strongly supported (pp = 1) as the sister group of the clade formed by *Synapturanus* + *Otophryne* (i.e. Otophryninae). The relationships between the clade formed by our three focal genera and the other microhylids (included as outgroups) are all strongly supported. The analysis undertaken on the nuDNA dataset separately led to a similar topology, with incongruences limited to poorly supported relationships (Supporting Information, Fig. S1).

Inference of ancestral areas using BioGeoBEARS favoured the DIVA+J model (Supporting Information, Table S12) and suggested that the clade *Adelastes* + Otophryninae started to diversify during the early Cenozoic, mean age 55 Mya (95% highest posterior distribution 51.4–58.8 Mya) in the Guiana Shield (also supported by models without the J parameter). This was also the case of the subsequent divergence between *Otophryne* and *Synapturanus*, which dated back to 46.1 Mya (42.3–49.7 Mya). *Adelastes* contained only two lowland species (*sensu* Kok, 2013), which diverged ~21.1 Mya (13.4–29.2 Mya). The diversification of *Otophryne* was also centred in Pantepui and started during the Miocene (15.9 Mya; 13.6–18.4 Mya). Subsequently, this group is most likely to have dispersed into the Eastern

species delimitation (IT), is illustrated by the use of coloured columns. Absence of available data for some species is indicated by 'NA'. B, principal components analysis (PCA) based on 12 external body measurements of 65 *Synapturanus* specimens (PC2 × PC3, size-corrected analyses and respective statistics are available in Supporting Information, Fig. S3). C, PCA based on three call variables from 44 recorded males of *Synapturanus* (statistics are available in Supporting Information, Table S8). Abbreviations: CCS, confirmed candidate species; UCS, unconfirmed candidate species. Consistent colour coding indicates species identity in A–C.

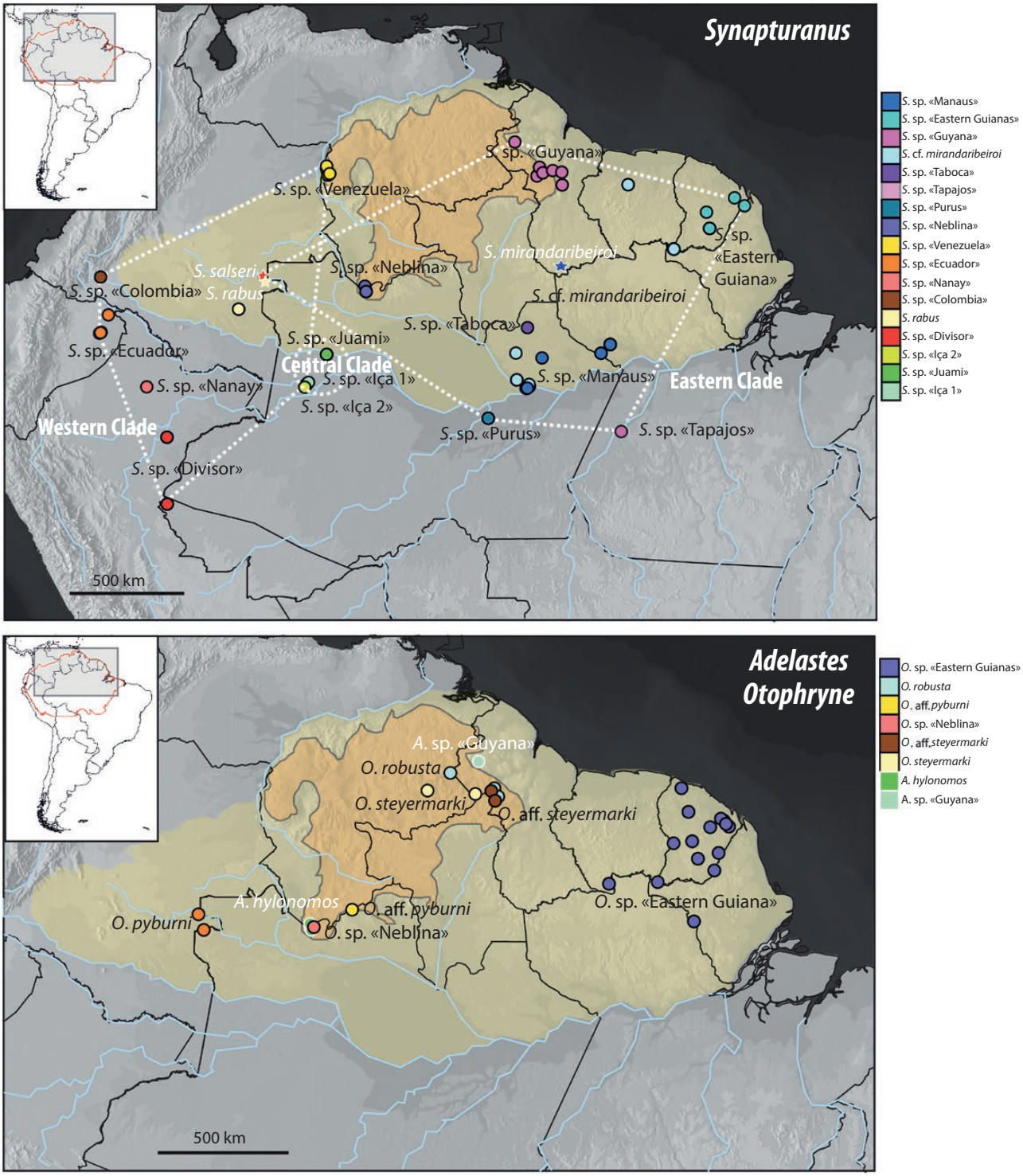

Figure 2. Maps of northern South America showing the distribution of the sampled material colour coded as in Figure 1 according to the species delimitation. The Guiana Shield region *s.l.* is delimited in yellow shading and the Pantepui region in orange. Topotypical *Synapturanus* samples are indicated with stars, and white dotted lines circumscribe the three major clades. The red outline in the inset map demarks Amazonia *sensu* Olson *et al.* (2001).

Guiana Shield during the Late Miocene after 9.3 Mya, giving rise to *Otophryne* sp. 'Eastern Guianas'.

The diversification of extant *Synapturanus* initiated ~31.4 Mya (27.1–33.5 Mya) during the late Palaeogene, either in the Western Guiana Shield or in Western Amazonia (Fig. 3; Supporting Information, Fig. S5). The initial divergence corresponded to that between the Central and the Western + Eastern Amazonia clades. Subsequently, during the Miocene, the Western clade probably dispersed southwards into Western Amazonia (Ecuador, Peru and Acre), while the Eastern Clade dispersed eastwards into the lowlands of the Eastern Guiana Shield. In relatively recent times, during the Pliocene, *Synapturanus* dispersed from the Eastern Guiana Shield into the region south of the Amazon River (margins of the Purus and the Tapajós). This clade experienced pronounced morphological diversification, notably in body size (Fig. 1B; Supporting Information, Table S3), but also in limbs and other traits related to fossoriality.

Shape analysis

Principal components analyses on 3D osteological data

The first three components from the PCA on cranial shape accounted for 64.1% of the overall variation (PC1 = 39.5%, PC2 = 14.2% and PC3 = 10.7%). PC1 captured mostly the relative length of the skull (*O. robusta* has a large cranium with a broad snout, whereas, at the other extreme, *Synapturanus* sp. 'Ecuador' has a relatively small cranium with a thin and pointed snout). PC2 captured mostly the variation in length of the squamosal, with minor contributions from the prootic width and snout length (*Otophryne* + *Synapturanus* showed marked differences in this axis relative to *Adelastes*). The three focal genera, *Adelastes*, *Otophryne* and *Synapturanus*, occupied distinct positions of the morphospace described by the first two PCs (Fig. 4A). *Adelastes* was positioned with all the other microhylids in an intermediate position along PC1. Nevertheless, the fossorial *Xenorhina* and *Myersiella* occupied intermediate positions in the morphospace, placed between *Synapturanus* and the other microhylids. Species of *Synapturanus* were distributed along PC2 according to their phylogenetic proximity, with species of the Eastern clade positioned on the negative part of the axis, while species of the Central and Western clades were distributed along the positive part (Fig. 4A). The three other species of the Eastern clade (*Synapturanus* sp. 'Guyana', *S. salseri* and *Synapturanus* sp. 'Neblina') were positioned between the Eastern and Western clades (Supporting Information, Fig. S6A).

The first three PCs performed on humeral shape explained 87.4% of the overall variation (PC1 = 73.8%, PC2 = 7.8% and PC3 = 5.7%). Most of the differences in shape were apparent along PC1, which segregates *Otophryne* and *Adelastes* from the Western clade of *Synapturanus* (Fig. 4B). Differences associated with PC1 tended to separate two types of humeral shape among *Synapturanus* species: species on the negative part of PC1 display a slender humerus with smaller distal articulation and a less developed deltopectoral crest (Fig. 4B), whereas species on the positive side of PC1 are characterized by a relatively robust humerus with a large distal articulation and well-developed deltopectoral crest. The non-fossorial and semi-fossorial microhylids were distributed along the negative part of PC1 (= slender humerus). The Central clade of *Synapturanus* occupied an intermediate position in PC1 along with the westernmost species of the Eastern clade and *Xenorhina*. The positive part of PC1 (= robust humerus) was occupied by the easternmost species of *Synapturanus*, which clustered together with highly specialized fossorial microhylids (*Barygenys*, *Myersiella* and *Elachistocleis*; Fig. 4B; Supporting Information, Fig. S6B).

Covariation between cranial and humeral shape in Synapturanus

Phylogenetic two-block partial least squares showed significant covariation between cranial and humeral shape within *Synapturanus* (R = 0.91; $P = 0.001$), with the first axis accounting for 94.2% of the covariation. Species distribution along both axes was in overall accordance with the phylogenetic relationships and biogeographical patterns (Fig. 4C; Supporting Information, Fig. S6C). Species clustered in three phenotypic groups: at one extreme, phenotype 1 is characterized by a relatively slender humerus with less developed deltopectoral crest and articulations and a less ossified cranium and is found in species of the Western clade of *Synapturanus*; at the other extreme, phenotype 3 corresponds to a relatively robust humerus with large crest and articulation, in addition to a relatively more ossified cranium with a larger prootic, larger squamosal and broader snout and is found in the easternmost species of the Eastern clade. An intermediate phenotype 2 included species of the Central and Eastern clades of *Synapturanus* (*S. salseri*, *Synapturanus* sp. 'Neblina' and *Synapturanus* sp. 'Guyana'). Covariation patterns were still significant when taking into account phylogeny (R = 0.92; $P = 0.01$).

DISCUSSION

Species diversity

Almost all of the studies that have explored the question of how many species of amphibians exist in Amazonia have uncovered high numbers of unnamed

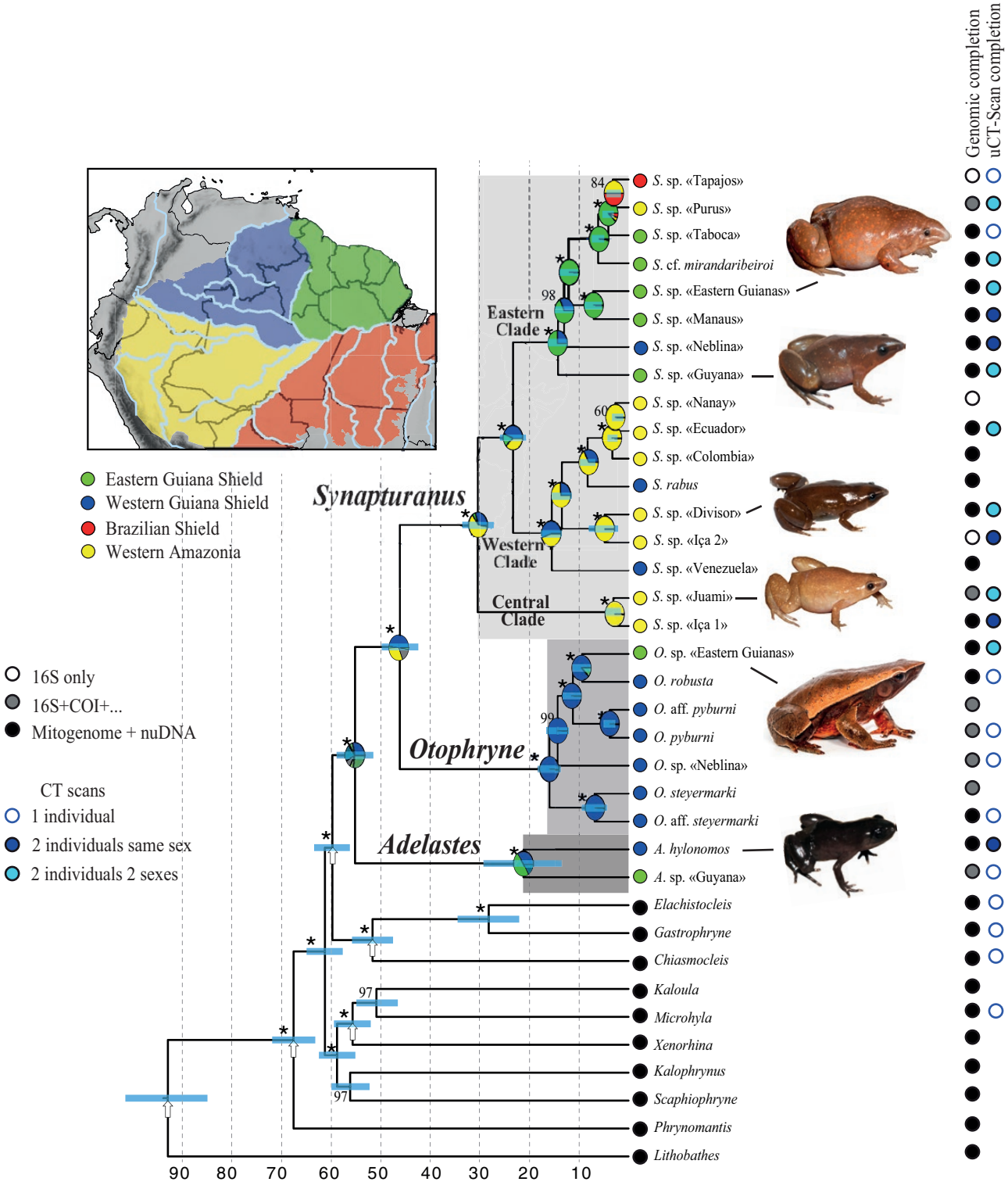

Figure 3. Maximum clade credibility chronogram inferred in BEAST 2 based on mitogenomic and nuclear DNA, and ancestral areas for the clade *Adelastes* + Otophryninae inferred in BIOGEOBEARS under the DIVA+J model (results of the DIVA model are available in Supporting Information, Table S12). Nodes with maximum posterior probability are indicated with an asterisk. Calibrated nodes are indicated with a small white arrow. Node bars indicate the 95% highest

species. These cases often correspond to populations that were previously considered to belong to species with wide distributions (e.g. Fouquet *et al.*, 2014; Gehara *et al.*, 2014; Carvalho *et al.*, 2020; Jaramillo *et al.*, 2020; Vacher *et al.*, 2020). This situation is strikingly exemplified in our results for *Synapturanus*, with a sixfold increase in species richness and, to a lesser extent, within *Otophryne* and *Adelastes*, for which a twofold increase was found. Interestingly, interspecific genetic distances among closely related OTUs with a commonly used 16S rDNA locus (Supporting Information, Table S8) are lower than 3–4% in several instances. This threshold in 16S rDNA distances has frequently been suggested to be indicative of candidate species in anurans (Fouquet *et al.*, 2007; Vieites *et al.*, 2009). Nonetheless, given the congruence across the three DNA-based methods, the recovered morphological and acoustic variation across populations, congruent nuDNA divergence and the rather ancient divergence estimated (> 3 Mya) among taxa, we argue that the resulting delimitation is meaningful. The use of single genetic marker distance criteria might result in a proportion of false negatives and should be used only with the necessary precautions in species delimitation. Instead, we advocate integrative approaches that combine both genetic and phenotypic (including bioacoustics) data (Padial *et al.*, 2010).

Importantly, our results also highlight that none of the currently recognized species geographical ranges is accurate. Almost all populations previously reported as belonging to a nominal species, and almost all newly sampled populations, belong to unnamed species. Moreover, it is likely that many additional species remain unsampled, notably *Otophryne* and *Adelastes* in the Pantepui region and *Synapturanus* in Western Amazonia. This particularly striking example of cryptic diversity exemplifies the limitations and difficulties in collecting these highly fossorial and secretive species, the resulting scarcity of available material in zoological collections and the logistical challenges associated with undertaking fieldwork in remote Amazonian regions.

The discovery of unnamed species and of phenotypically differentiated populations previously reported as a single species in Amazonia is thus not surprising, particularly in fossorial groups. However, the newly identified lineages are unexpectedly old, as is the case for our three focal genera, which display crown ages between 30 and 15 Mya. Divergences dating back to the Miocene have been reported for unnamed lineages within *Adelophryne* (Fouquet *et al.*, 2012), *Adenomera* (Fouquet *et al.*, 2014) and *Stefania* (Kok *et al.*, 2017), and even back to the Oligocene for *Amazophrynella* (Rojas *et al.*, 2018). These examples illustrate how knowledge gaps in Amazonia can hamper biogeographical inferences at the regional scale. Preliminary species-level investigations, such as the one presented herein, are therefore required to shed light on the historical causes and regional determinants of the outstanding diversity of this region.

Another result with potential taxonomic implications is the sister relationship between *Adelastes* and Otophryninae. The phylogenetic position of *Adelastes* had recently been established using phylogenomic data (Peloso *et al.*, 2016; Hime *et al.*, 2021). Tu *et al.* (2018) found contentious the phylogenetic position of *Adelastes* as the sister group of Otophryninae found by Peloso *et al.* (2016), but this position was confirmed by Hime *et al.* (2021) without further discussion of the taxonomic implications of this relationship. Although outside of the scope of our study, this sister relationship raises the question of the pertinence of keeping the monotypic subfamily Adelastinae instead of assigning *Adelastes* to Otophryninae.

Historical biogeography

The geographical centre of diversification of most Neotropical groups remains difficult to infer, not only because of putative extinctions but also because of subsequent dispersals and intense landscape dynamics leading to the reshuffling of the spatial distribution of organisms throughout the Cenozoic. Consequently, our ability to investigate the spatial origins of focal groups is usually restricted to the Neogene, but often to even more recent periods (Smith *et al.*, 2014; da Silva *et al.*, 2019; Cracraft *et al.*, 2020), depending on the intensity of these dispersal events throughout the Neotropics. The 55-Myr-old clade formed by *Adelastes* and Otophryninae represents a rare and striking example of the role of the Guiana Shield as a source in the diversification of the Neotropical biota during the early Cenozoic.

South America has drifted little latitudinally over the past 100 Myr, and its northern part has remained predominantly tropical (Hammond, 2005). Anchored

posterior distribution of node dates. Coloured circles on the tips of the tree indicate the geographical distribution of sampled operational taxonomic units. Pie charts on nodes show the proportion of most likely ancestral areas. Colours of node pie charts correspond to the geographical areas shown in the map. Molecular data completeness and sampling of three-dimensional micro-computed tomography scans are indicated on the right of the figure. Some examples of the morphological variation of the target genera are depicted (not to scale).

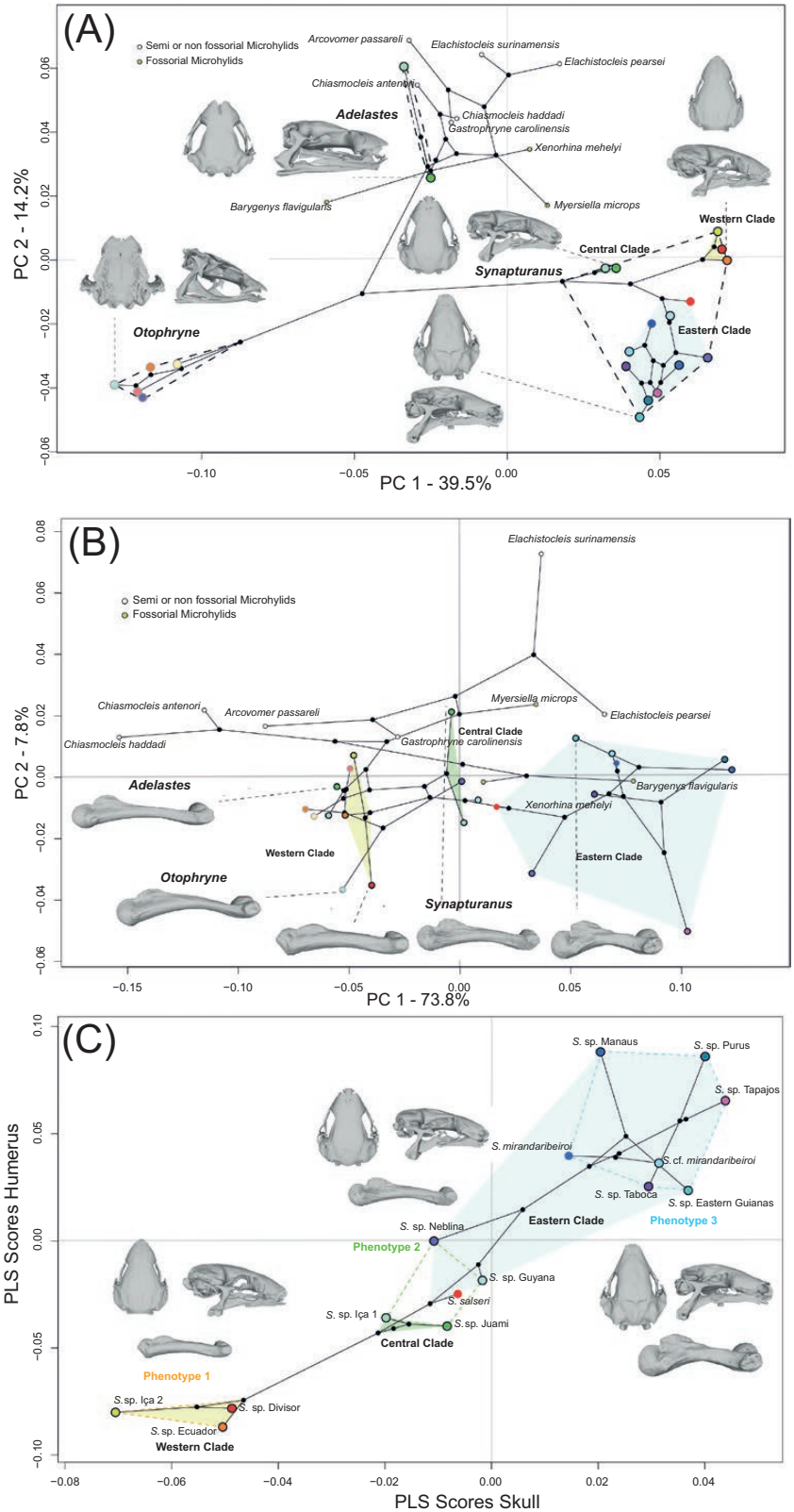

Figure 4. Cranial and humeral shape variation. A, phylomorphospace defined by the first two principal components (PCs) of cranial shape, which described 53.7% of the total variation. Dotted lines indicate the distinct target genera. B,

on its craton, the Guiana Shield has remained comparatively stable geologically throughout the Cenozoic, unlike the predominantly sedimentary and dynamic western part of the continent, notably Western Amazonia (Hoorn *et al.*, 2010). Relative climatic and geological long-term stability and the existence of marked elevational gradients might explain why the Western Guiana Shield acted as a source of diversity for the surrounding areas in *Adelastes* + Otophryninae and, possibly, in many other groups. However, to our knowledge, available examples of groups having their origin in the Pantepui region and that have diversified either in the tepuis (highlands) or in Amazonia (lowlands) display younger crown ages.

In Amazonian amphibians, there are few compelling examples of centres of diversification from the Early Neogene being regionally circumscribed, such as the ones documented herein for *Synapturanus* and *Otophryne* (but for *Allobates*, see Réjaud *et al.*, 2020; and for the Guiana Shield clade of *Adelophryne*, see Fouquet *et al.*, 2012), which probably also originated in the Guiana Shield. This is also assumed to be the case of the frog clade Cophomantini (Pinheiro *et al.*, 2019), the caecilians *Microcaecilia* and *Rhinatrema–Epicrionops* (San Mauro *et al.*, 2014) and several plant families, such as Bromeliaceae and Rapateaceae (Givnish *et al.*, 2011). Mountainous areas, such as the Pantepui region, might have favoured the persistence of lineages over the last 23 Mya, as has been the case for the numerous clades endemic to the tepui highlands (e.g. Kok *et al.*, 2017, 2018). The diversification within *Otophryne* possibly involved long-term persistence on mountains, because the lowland lineages (e.g. *Otophryne* sp. 'Eastern Guianas' and *O. pyburni*) have apparently dispersed more recently (~10 Mya) into the eastern and the western lowlands. The three genera studied herein comprise both lowland and upland species, which highlights the importance of elevational gradients in the diversification of both highland (> 1500 m a.s.l.) and lowland biota in the Pantepui region.

Diversification within *Synapturanus* is complex, because our biogeographical inferences suggested three possible independent dispersal events from the Western Guiana Shield into Western Amazonia and one towards the Eastern Guiana Shield. The dispersal and diversification of *Synapturanus* throughout Amazonia might have been influenced by the Pebas system, a lacustrine ecosystem occupying most of Western Amazonia from the early Miocene (23 Mya) until 10–9 Mya (Hoorn *et al.*, 2010, 2017). From 9 Mya onwards, this system started to drain eastwards into the Atlantic Ocean, but lacustrine ecosystems (the Acre system) still occupied the region until ~5 Mya. This region corresponds to a large portion of what we currently consider as Western Amazonia (Albert *et al.*, 2018), and thus it can be assumed to have become suitable for terrestrial species only in recent times. The species occurring in the region previously occupied by the Pebas system in Western Amazonia (e.g. *Synapturanus* sp. 'Içá 1' and sp. 'Içá 2', *Synapturanus* sp. 'Juami') might have dispersed either before this system was established or after it dried out (i.e. from surrounding areas after the conversion of lacustrine ecosystems to *terra-firme* during the Pliocene; Albert *et al.*, 2018). The influence of these hydrological changes on anuran biogeography has been suggested previously for several groups of anurans (Pirani *et al.*, 2020; Réjaud *et al.*, 2020). If these dispersals have occurred before, these species might have been limited to the eastern margins of the Pebas system (*Synapturanus* sp. 'Divisor' and *Synapturanus* sp. 'Içá 2'). However, dispersals from the Western Guiana Shield into Western Amazonia might have taken place after 10 Mya, with the hydrological shift to a system draining eastwards and the drying of the Pebas system. Subsequently, the remaining species of the Western clade seem to have diversified along the Andean foothills and, secondarily, dispersed back into the Guiana Shield (*S. rabus*) after the establishment of the modern Amazon hydrological system. Notably, this diversification in Western Amazonia is associated with the acquisition of a particular phenotype characterized by slender crania and humeri.

The centre of origin of the Eastern clade remains ambiguous, complicated by the unknown phylogenetic position of *S. salseri*, although this species probably diverged early within that clade. Nevertheless, the origin of this clade is likely to be centred in the lowlands of Pantepui (Fig. 2). From there, it dispersed into the Eastern Guiana Shield (~13 Mya) and acquired a novel phenotype, characterized by heavily modified crania and humeri. This event is followed by the most recent dispersal of this clade southwards across the Amazon River (*Synapturanus* sp. 'Purus' and *Synapturanus* sp. 'Tapajós' ~4 Mya). A similar

phylomorphospace defined by the first two principal components of humeral shape, which described 81.6% of the total variation. Full labels for the same figures are available in the Supporting Information (Fig. S6). C, scatter plot of the first two-block partial least squares analysis (2B-PLS) axes for *Synapturanus*. The two axes captured 94.17% of the total shape covariation between the cranium and the humerus. Circles are colour coded by species according to the previous figures. Colour-filled polygons in all panels indicate the three major clades within *Synapturanus*; black lines represent phylogenetic relationships, and dotted coloured lines in C indicate the inferred distinct phenotypes.

route and divergence times are also recovered in other amphibian groups or species pairs (e.g. *Allobates*; Réjaud *et al.*, 2020). Unravelling divergence and dispersal patterns of fossorial *terra-firme* organisms can help to reconstruct recent neotectonic interfluvial rearrangements and drainage captures resulting in exchanges in land masses (e.g. the one suggested in the formation of the lower Negro River; Almeida-Filho & Miranda, 2007), and our results seem to corroborate these patterns.

Shape evolution of the cranium and humerus in *Synapturanus*

Patterns of variation of in the shape of the cranium and humerus in *Synapturanus* are largely concordant with biogeographical patterns, but not fully with its phylogenetic history. The evolution of the shape of both structures resulted in the acquisition of three phenotypes. When interpreting these morphological results in the light of their phylogeny, we can hypothesize that phenotype 2 might represent the plesiomorphic state, whereas phenotypes 1 and 3 have been derived from it ~13 and 12 Mya, coinciding with dispersal events into Western Amazonia and the Eastern Guiana Shield, respectively. Therefore, morphological divergence associated with dispersal into new regions might reflect adaptation to new habitats. For instance, nearly all the species harbouring phenotype 3 (with robust humeri) occur on Ferralsols derived from long-term erosion of the craton (2.5–2 Gya; Supporting Information, Fig. S7). In contrast, species with phenotype 1 (large eyes, slender) are found only in Acrisols or clay-rich subsoils, which have been deposited by avulsive fluvial and lacustrine belts in floodplain environments in lowland Amazonia during the Miocene (23–10 Mya). Finally, the species showing the putatively plesiomorphic phenotype 2 tend to be associated with a larger range of soil types, such as Plinthosols, Acrisols and Leptosols (Quesada *et al.*, 2011; Supporting Information, Fig. S7). Taken together, the differences in humeral and cranial shapes observed in different groups of *Synapturanus* might represent distinct fossorial modalities, in which the associated traits potentially represent adaptations to soils with distinct properties. Future tests of this hypothesis will rely on a more precise characterization of the soil types and a better understanding of the species distributions that would allow for a thorough statistical evaluation of the relative importance of these environmental drivers.

Bones allow movement and need to respond to and resist muscular forces while supporting loads (Hildebrand, 1985). As such, bones are shaped by force and motion, and their form is likely to be closely related to the movements executed and, by inference, also to the ecology of an organism (Ricklefs & Miles, 1994). Although many frogs share a conserved skull shape, several extreme forms have repeatedly evolved hyperossified structures, notably in relationship to fossorial lifestyles (Paluh *et al.*, 2020). In our study, the cranial shapes of three focal genera occupy remarkably distinct positions within the morphospace in comparison to those of other microhylids. This result is likely to be related to the drastic ecological and behavioural divergences among them, particularly *Otophryne* and *Synapturanus*, which contrast with the typical semi-fossorial phenotype of *Adelastes*. Likewise, Vidal-García & Keogh (2017) found that skull shape diversity in Myobatrachidae was phylogenetically conserved and correlated with diet, whereas limb shape evolved convergently in association with diet, locomotion and burrowing behaviour. Moreover, extreme skull shapes in frogs characterized by a pointed snout, anteriorly shifted jaw point and reduced squamosal are believed to be driven by myrmecophagous diet rather than fossoriality (Vidal-García & Keogh, 2017; Paluh *et al.*, 2020). One of the limitations of our study is the lack of information on diet, locomotion and the burrowing behaviour for almost all the species in these genera. Nevertheless, *Synapturanus* species are probably myrmecophagous specialists (Nelson & Lescure, 1975; Pyburn, 1975, 1977), and the variation in skull shape demonstrated here might thus be explained by distinct degrees of diet specialization.

However, these macroscale features are much less evident with the humerus, which varies more at a shallower evolutionary scale. This is illustrated in *Synapturanus*, whose cranial evolution is more in accordance with the phylogeny, whereas the humeral shape of the western species of the Eastern clade is more similar to that of the Central clade than to their eastern relatives. This different signal and discrepancy with the phylogeny could suggest a higher lability of the humerus in response to a fossorial lifestyle. Keeffe & Blackburn (2020) demonstrated that the humeri of most forward-burrowing frogs are morphologically distinct from those of non-forward burrowers. This includes features such as a curved and thick diaphysis, the presence of a pronounced ventral crest, and relatively large epicondyles and humeral head. They included *S. mirandaribeiroi* (phenotype 3), and these characteristics clearly match the other related species. However, the humeri of the *Synapturanus* species displaying other phenotypes do not fit this description, which leads us to hypothesize that forward-burrowing behaviour might not be shared by all *Synapturanus*. The proportionally larger eye of the species of the Western clade (phenotype 1), already noticed by Pyburn (1977) and observed along PC2 (Supporting Information, Fig. S4), and through personal field observations, also suggests more epigean habits in

species sharing phenotypes 2 and 3. It is likely that *Synapturanus* of the Western clade forage in the leaf litter, whereas Eastern *Synapturanus* not only reproduce but also forage underground, thus requiring adapted crania and limbs.

Study of these enigmatic frogs is challenging, and the lack of natural history observations renders these aforementioned hypotheses largely speculative. Further research should focus not only on natural history observations but also on habitat characterization, acoustic recordings, documenting additional populations and species descriptions. The conservation status of many of the species documented herein remains data deficient and, considering their putatively small ranges, some might be under severe risk of extinction. We hope that this study will encourage and stimulate further research in these areas.

ACKNOWLEDGEMENTS

This study benefited from an 'Investissement d'Avenir' grant managed by the Agence Nationale de la Recherche (CEBA, ref. ANR-10-LABX-25-01) and from the French Foundation for Research on Biodiversity (FRB) and its partners (https://www.fondationbiodiversite.fr/ PMAST-SOR-2018-4). We also acknowledge support from the French/Brazilian GUYAMAZON program action (IRD, CNRS, CTG, CIRAD and Brazilian Fundação de Amparo à Pesquisa do Estado do Amazonas-FAPEAM 062.00962/2018), Conselho Nacional de Desenvolvimento Científico e Tecnológico (CNPq #140716/2016-5; 305535/2017-0; PQ 302501/2019-3; PQ 303070/2017-0), Fundação de Amparo à Pesquisa do Estado de São Paulo (FAPESP: 2003/10335-8, 2012/15754-8, 2011/50146-6; and NSF-FAPESP and NASA Dimensions of Biodiversity Program, grant numbers: BIOTA 2013/50297-0, NSF-DEB 1343578), SENESCYT (Arca de Noé Initiative), the L'Oréal-UNESCO For Women In Science Program, the Fonds voor Wetenschappelijk Onderzoek (FWO12A7614N and FWO12A7617N), Deutsche Forschungsgemeinschaft (DFG; ER 589/2-1) and Research Program INV-2017-51-1432 from the School of Sciences, Universidad de los Andes. We are grateful to Jean-Pierre Vacher, Amaia Iribar-Pelozuelo, Phillip Lenktaitis, Juliana Naomi Tanaka, Jean Dumoncel, Antonio Mollo Neto, Quentin Martinez, Renaud Lebrun, Pierre-Henri Fabre and Omar Rojas Padilla for their help in the laboratory and with scans. The 3D data acquisitions were performed using the micro-computed tomography facilities of the magnetic resonance imaging platform member of the national infrastructure France-BioImaging [supported by the French National Research Agency (ANR-10-INBS-04, 'Investments for the future') and by the Labex CEMEB (ANR-10-LABX-0004) and NUMEV (ANR-10-LABX-0020)] and American Museum of Natural History's Microscopy and Imaging Facility (we thank H. Towbin and M. Hill for help with acquiring and processing data). We also thank Annemarie Ohler, J. Celsa Señaris, María Matilde Aristeguieta, Mark Wilkinson, David Gower, FNJV, Macaulay, Addison Wynn, MNHN, collections of Amphibians and Reptiles (INPA-H) and Genetic Resources (INPA-HT) of INPA, and Dave Blackburn for helping with specimen loans and data. Additional thanks go to Jhon Jairo López-Rojas, Elodie Courtois, Mael Dewynter, Michel Blanc, Benoit Villette, Philippe Gaucher, Morley Read, Rawien Jairam, Paul Ouboter, Sebastien Cally, Lucéia Bonora, Jucivaldo Lima, Mauro Teixeira Jr, Marco Sena, Pedro Dias, Jerriane Gomes, Felipe Magalhães, André Amaral Nogueira, Sebastien Barrioz, Quentin Rome, Timothe Colston, Andrew Snyder and Brice Noonan for their contribution in collecting calls and specimens. Part of the collected material come from expedition undertaken with the 'Parc Amazonien de Guyane', notably during the 'Our Planet Reviewed' Guyane-2015 expedition in the Mitaraka range organized by the MNHN and Pro-Natura international. Permits for collection (MinAmb for Venezuela: #4156 and #5179) and for access to genetic resources (#0076; February 22, 2011; Natuurbeheer Suriname STINASU for Suriname). Fieldwork in the Tapajós region received financial and logistical support by CNEC WorleyParsons Engenharia SA. Peruvian material was authorized by RGD#152-2018-MINAGRI/SERFOR-DGGSPFFS. The expedition to ESEC Juami-Japurá was funded with grants from Programa de Excelência Acadêmica of Coordenação de Aperfeiçoamento de Pessoal de Nível Superior (PROEX- CAPES, project #1030/2014), with additional funds from Programa de Áreas Protegidas of Instituto Chico Mendes de Conservação da Biodiversidade (ARPA/ICMBio). Fieldwork in Guyana was supported by the Iwokrama International Centre and R. Thomas, GFC-PRDD with permissions to conduct biodiversity research from EPA Guyana. We thank Elder Pena and the ICMBio staff in Tefé for logistical support and for making our trip to the Juami River possible. RAN/ICMBio and ESEC Juami-Japurá/ICMBio provided collecting permits (license #57090-1). We would also like to thank Paulo Muzy from the University of São Paulo, the Yanomami people of Maturacá, and General Mayer who, through the financial and logistical support of the Brazilian Army, made the Expedition to Pico da Neblina possible. V.T.C. thanks Coordenação de Aperfeiçoamento de Pessoal de Nível Superior – CAPES (PNPD). Finally, we warmly thank John A. Allen (BJLS Editor), Jeff Streicher, Mark D. Scherz and the two anonymous reviewers for their thorough

examination of our manuscript, which was greatly improved thanks to them.

AUTHORS' CONTRIBUTIONS

A.F., conception and design, acquisition, analysis and interpretation of data and manuscript writing; K.L., acquisition, analysis and interpretation of data and manuscript revision; M.F., acquisition and analysis of data and manuscript revision; A.R., acquisition, analysis and interpretation of data and manuscript revision; I.P., S.M., U.S., S.B., M.T.R., S.C.-F., P.L.V.P., L.J.C.L.M., R.R., S.M.S., F.D.V., A.C., J.M.G., F.J.M.R.-R., G.G.-U., V.T.C., M.G., M.M., P.J.R.K., T.H., F.W., A.J.C., S.R., J.J.M.-C., R.R.R.Z., D.P., P.I.S., R.E. and A.-C.F., conception and design, acquisition, analysis and interpretation of data, manuscript writing.

REFERENCES

Adams D, **Collyer M**, **Kaliontzopoulou A. 2019.** *geomorph: geometric morphometric analyses of 2D/3D landmark data (OpenGL) (R package version 3.2)*. https://cran.r-project.org/web/packages/geomorph/index.html

Adler D, **Murdoch D. 2012.** *rgl: 3D visualization device system (OpenGL) (R package version 0.92)*. https://cran.r-project.org/web/packages/rgl/index.html

Albert JS, **Val P**, **Hoorn C. 2018.** The changing course of the Amazon River in the Neogene: center stage for Neotropical diversification. *Neotropical Ichthyology* **16:** e180033.

Almeida AP, **de Carvalho VT**, **Gordo M**, **Rojas ZR**, **Menin M. 2014.** First record of *Adelastes hylonomos* Zweifel, 1986 (Amphibia, Anura, Microhylidae) outside the type locality, with notes on the advertisement call. *Check List* **10:** 1226–1228.

Almeida-Filho R, **Miranda FP. 2007.** Mega capture of the Rio Negro and formation of the Anavilhanas Archipelago, central Amazônia, Brazil: Evidences in an SRTM digital elevation model. *Remote Sensing of Environment* **110:** 387–392.

Antonelli A, **Zizka A**, **Carvalho FA**, **Scharn R**, **Bacon CD**, **Silvestro D**, **Condamine FL. 2018.** Amazonia is the primary source of Neotropical biodiversity. *Proceedings of the National Academy of Sciences of the United States of America* **115:** 6034–6039.

Audacity Team. **2020.** *Audacity(R): free audio editor and recorder [computer application]*, *Version 2.4.1*. https://www.audacityteam.org/

Barrio-Amorós CL, **Rojas-Runjaic FJM**, **Señaris JC. 2019.** Catalogue of the amphibians of Venezuela: illustrated and annotated species list, distribution, and conservation. *Amphibian & Reptile Conservation* **13:** 1–198.

Bouckaert R, **Heled J**, **Kühnert D**, **Vaughan T**, **Wu C-H**, **Xie D**, **Suchard MA**, **Rambaut A**, **Drummond AJ. 2014.** BEAST 2: a software platform for Bayesian evolutionary analysis. *PLoS Computational Biology* **10:** e1003537.

Boulenger GA. 1900. Batrachians. In E. R. Lankester, Report on a collection made by Messrs. F.V. McConnell and J.J. Quelch at Mount Roraima in British Guiana. *Transactions of the Linnean Society of London, 2nd series, Zoology* **8:** 55–56.

Campbell JA, **Clarke BT. 1998.** A review of frogs of the genus *Otophryne* (Microhylidae) with the description of a new species. *Herpetologica* **54:** 301–317.

Campbell V, **Lapointe F-J. 2009.** The use and validity of composite taxa in phylogenetic analysis. *Systematic Biology* **58:** 560–572.

Carvalho TRD, **Moraes LCJL**, **Lima AP**, **Fouquet A**, **Peloso PLV**, **Pavan D**, **Drummond LO**, **Rodrigues MT**, **Giaretta AA**, **Gordo M**, **Neckel-Oliveira S**, **Haddad CFB. 2020.** Systematics and historical biogeography of Neotropical foam-nesting frogs of the *Adenomera heyeri* clade (Leptodactylidae), with the description of six new Amazonian species. *Zoological Journal of the Linnean Society* zlaa051.

Carvalho VT, **Bonora L**, **Vogt RC. 2007.** Geographic distribution: *Otophryne pyburni*. *Herpetological Review* **38:** 349.

Castroviejo-Fisher S, **Koehler J**, **De La Riva I**, **Padial JM. 2017.** A new morphologically cryptic species of *Phyllomedusa* (Anura: Phyllomedusidae) from Amazonian forests of northern Peru revealed by DNA sequences. *Zootaxa* **4269:** 245–264.

Cracraft J, **Ribas CC**, **d'Horta FM**, **Bates J**, **Almeida RP**, **Aleixo A**, **Boubli JP**, **Campbell KE**, **Cruz FW**, **Ferreira M**, **Fritz SC**, **Grohmann CH**, **Latrubesse EM**, **Lohmann LG**, **Musher LJ**, **Nogueira A**, **Sawakuchi AO**, **Baker P. 2020.** The origin and evolution of Amazonian species diversity. In: Rull V, Carnaval AC, eds. *Neotropical diversification: patterns and processes*. Cham: Springer, 225–244.

Drummond AJ, **Ho SYW**, **Phillips MJ**, **Rambaut A. 2006.** Relaxed phylogenetics and dating with confidence. *PLoS Biology* **4:** e88.

Dupin J, **Matzke NJ**, **Särkinen T**, **Knapp S**, **Olmstead RG**, **Bohs L**, **Smith SD. 2017.** Bayesian estimation of the global biogeographical history of the Solanaceae. *Journal of Biogeography* **44:** 887–899.

Emerson SB. 1976. Burrowing in frogs. *Journal of Morphology* **149:** 437–458.

Ernst R, **Rödel M**, **Arjoon D. 2005.** On the cutting edge – the anuran fauna of the Mabura Hill Forest Reserve, central Guyana. *Salamandra* **41:** 179–194.

Ezard T, **Fujisawa T**, **Barraclough TG. 2009.** *Splits: species' limits by threshold statistics. R package version 1.29*. https://r-forge.r-project.org/R/?group_id=333

Feng Y-J, **Blackburn DC**, **Liang D**, **Hillis DM**, **Wake DB**, **Cannatella DC**, **Zhang P. 2017.** Phylogenomics reveals rapid, simultaneous diversification of three major clades of Gondwanan frogs at the Cretaceous–Paleogene boundary. *Proceedings of the National Academy of Sciences of the United States of America* **114:** E5864–E5870.

Fouquet A, **Cassini CS**, **Haddad CFB**, **Pech N**, **Rodrigues MT. 2014.** Species delimitation, patterns of diversification and historical biogeography of a Neotropical

frog genus; *Adenomera* (Anura, Leptodactylidae). *Journal of Biogeography* **41:** 855–870.

Fouquet A, **Gilles A**, **Vences M**, **Marty C**, **Blanc M**, **Gemmell NJ. 2007.** Underestimation of species richness in Neotropical frogs revealed by mtDNA analyses. *PLoS ONE* **2:** e1109.

Fouquet A, **Loebmann D**, **Castroviejo-Fisher S**, **Padial JM**, **Orrico VGD**, **Lyra M**, **Roberto IJ**, **Kok PJR**, **Haddad CFB**, **Rodrigues MT. 2012.** From Amazonia to the Atlantic forest: molecular phylogeny of Phyzelaphryninae frogs reveals unexpected diversity and a striking biogeographic pattern emphasizing conservation challenges. *Molecular Phylogenetics and Evolution* **65:** 547–561.

Fouquet A, **Vidal N**, **Dewynter M. 2019.** The amphibians of the Mitaraka massif, French Guiana. *Zoosystema* **41:** 359–374.

Frost DR. 2020. *Amphibian Species of the World: an online reference. Version 6.1*. New York: American Museum of Natural History. https://amphibiansoftheworld.amnh.org/

Gagliardi-Urrutia G, **Iglesias MO**, **Venegas PJ. 2015.** Amphibias and reptiles. In: Pitman N, Vriensendorp C, Chávez LR, Wachter T, Reyes DA, del Campo Á, Gagliardi-Urrutia G, González DR, Trevejo L, González DR, Heilpern S, eds. *Perú: Tapiche-Blanco. Rapid biological and social inventories report 27*. Chicago: The Field Museum, 117–125.

Gehara M, **Crawford AJ**, **Orrico VG**, **Rodríguez A**, **Lötters S**, **Fouquet A**, **Barreintos LS**, **Brusquetti F**, **De la Riva I**, **Ernst R**, **Gagliardi-Urrutia G**, **Glaw F**, **Guayasamin JM**, **Hölting M**, **Jansen M**, **Kok PJR**, **Kwet A**, **Lingnau R**, **Lyra M**, **Moravec J**, **Pombal JP Jr**, **Rojas-Runjaic FJM**, **Schulze A**, **Señaris JC**, **Solé M**, **Rodrigues MT**, **Twomey E**, **Haddad CFB**, **Vences M**, **Köhler J. 2014.** High levels of diversity uncovered in a widespread nominal taxon: continental phylogeography of the Neotropical tree frog *Dendropsophus minutus*. *PLoS ONE* **9:** e103958.

Givnish TJ, **Barfuss MH**, **Van Ee B**, **Riina R**, **Schulte K**, **Horres R**, **Gonsiska PA**, **Jabaily RS**, **Crayn DM**, **Smith JAC**, **Winter K. 2011.** Phylogeny, adaptive radiation, and historical biogeography in Bromeliaceae: insights from an eight-locus plastid phylogeny. *American Journal of Botany* **98:** 872–895.

Gordo M, **Knell G**, **Rivera Gonzales DE. 2006.** Amphibians and reptiles. In: Vriesendorp C, Pitman N, Rojas Moscoso JI, Pawlak BA, Rivera Chavez L, eds. *Peru: Matses. Rapid biological inventories report 16*. Chicago: The Field Museum, 191–196.

Hammond DS. 2005. *Tropical forests of the Guiana Shield: ancient forests in a modern world*. Cambridge: CABI Publishing.

Hildebrand M. 1985. Walking and running. In: Hildebrand M, Bramble DM, Liem KF, Wake DB, eds. *Functional vertebrate morphology*. Cambridge: Harvard University Press, 38–57.

Hime PM, **Lemmon AR**, **Moriarty LEC**, **Prendini E**, **Brown JM**, **Thomson RC**, **Kratovil JD**, **Noonan BP**, **Pyron RA**, **Peloso PLV**, **Kortyna ML**, **Keogh JS**, **Donnellan SC**, **Lockridge MR**, **Raxworthy CJ**, **Kunte K**, **Ron SR**, **Das S**, **Gaitonde N**, **Green DM**, **Labisko J**, **Che J**, **Weisrock DW. 2021.** Phylogenomics reveals ancient gene tree discordance in the amphibian tree of life. *Systematic Biology* syaa034.

Hoorn C, **Bogotá-A GR**, **Romero-Baez M**, **Lammertsma EI**, **Flantua SGA**, **Dantas EL**, **Dino R**, **do Carmo DA**, **Chemale F Jr**. **2017.** The Amazon at sea: Onset and stages of the Amazon River from a marine record, with special reference to Neogene plant turnover in the drainage basin. *Global and Planetary Change* **153:** 51–65.

Hoorn C, **Wesselingh FP**, **ter Steege H**, **Bermudez MA**, **Mora A**, **Sevink J**, **Sanmartín I**, **Sanchez-Meseguer A**, **Anderson CL**, **Figueiredo JP**, **Jaramillo C**, **Riff D**, **Negri FR**, **Hooghiemstra H**, **Lundberg J**, **Stadler T**, **Särkinen T**, **Antonelli A. 2010.** Amazonia through time: Andean uplift, climate change, landscape evolution, and biodiversity. *Science* **330:** 927–931.

Jaramillo AF, **De la Riva I**, **Guayasamin JM**, **Chaparro JC**, **Gagliardi-Urrutia G**, **Gutiérrez R**, **Brcko I**, **Vilà C**, **Castroviejo-Fisher S. 2020.** Vastly underestimated species richness of Amazonian salamanders (Plethodontidae: *Bolitoglossa*) and implications about plethodontid diversification. *Molecular Phylogenetics and Evolution* **149:** 106841.

Jenkins CN, **Pimm SL**, **Joppa LN. 2013.** Global patterns of terrestrial vertebrate diversity and conservation. *Proceedings of the National Academy of Sciences of the United States of America* **110:** E2602–E2610.

Kapli P, **Lutteropp S**, **Zhang J**, **Kobert K**, **Pavlidis P**, **Stamatakis A**, **Flouri T. 2017.** Multi-rate Poisson tree processes for single-locus species delimitation under maximum likelihood and Markov chain Monte Carlo. *Bioinformatics* **33:** 1630–1638.

Katoh K, **Rozewicki J**, **Yamada KD. 2017.** MAFFT online service: multiple sequence alignment, interactive sequence choice and visualization. *Briefings in Bioinformatics* **20:** 1160–1166.

Kearney M. 2002. Fragmentary taxa, missing data, and ambiguity: mistaken assumptions and conclusions. *Systematic Biology* **51:** 369–381.

Keeffe R, **Blackburn DC. 2020.** Comparative morphology of the humerus in forward-burrowing frogs. *Biological Journal of the Linnean Society* **131:** 291–303.

Klaus KV, **Matzke NJ. 2020.** Statistical comparison of trait-dependent biogeographical models indicates that Podocarpaceae dispersal is influenced by both seed cone traits and geographical distance. *Systematic Biology* **69:** 61–75.

Köhler J, **Jansen M**, **Rodríguez A**, **Kok PJR**, **Toledo LF**, **Emmrich M**, **Glaw F**, **Haddad CFB**, **Rödel M-O**, **Vences M. 2017.** The use of bioacoustics in anuran taxonomy: theory, terminology, methods and recommendations for best practice. *Zootaxa* **4251:** 1–124.

Kok PJR. 2013. *Islands in the sky: species diversity, evolutionary history, and patterns of endemism of the Pantepui Herpetofauna*. Institute of Biology (IBL)/Nationaal Herbarium Nederland (NHN), Faculty of Science, Leiden University.

Kok PJR, **Kalamandeen M. 2008.** Introduction to the taxonomy of the amphibians of Kaieteur National Park, Guyana. *Abc Taxa* **5:** 1–278.

Kok PJR, **MacCulloch RD**, **Means DB**, **Roelants K**, **Van Bocxlaer I**, **Bossuyt F. 2012.** Low genetic diversity in tepui summit vertebrates. *Current Biology* **22:** 589–590.

Kok PJR, **Ratz S**, **MacCulloch RD**, **Lathrop A**, **Dezfoulian R**, **Aubret F. Means DB. 2018.** Historical biogeography of the palaeoendemic toad genus *Oreophrynella* (Amphibia: Bufonidae) sheds a new light on the origin of the Pantepui endemic terrestrial biota. *Journal of Biogeography* **45:** 26–36.

Kok PJR. Russo VG, **Ratz S**, **Means DB**, **MacCulloch RD**, **Lathrop A**, **Aubret F**, **Bossuyt F. 2017.** Evolution in the South American 'Lost World': insights from multilocus phylogeography of stefanias (Anura, Hemiphractidae, *Stefania*). *Journal of Biogeography* **44:** 170–181.

Landis MJ, **Matzke NJ**, **Moore BR**, **Huelsenbeck JP. 2013.** Bayesian analysis of biogeography when the number of areas is large. *Systematic Biology* **62:** 789–804.

Lanfear R, **Frandsen PB**, **Wright AM**, **Senfeld T**, **Calcott B. 2017.** PartitionFinder 2: new methods for selecting partitioned models of evolution for molecular and morphological phylogenetic analyses. *Molecular Biology and Evolution* **34:** 772–773.

Lê S, **Josse J**, **Husson F. 2008.** FactoMineR: an R package for multivariate analysis. *Journal of Statistical Software* **25:** 1–18.

Lima AP, **Magnuson WE**, **Menin M**, **Erdtmann LK**, **Rodrigues DJ**, **Keller C**, **Hödl W. 2006.** *Guia de sapos da Reserva Adolpho Ducke, Amazônia Central*. Manaus: Áttema Design Editorial.

López-Rojas JJ, **Cisneros-Heredia DF. 2012.** *Synapturanus rabus* Pyburn, 1977 in Peru (Amphibia: Anura: Microhylidae): filling gap. *Check List* **8:** 274–275.

MacCulloch RD, **Lathrop A**, **Minter LR**, **Khan SZ. 2008.** *Otophryne* (Anura: Microhylidae) from the highlands of Guyana: redescriptions, vocalisations, tadpoles and new distributions. *Papéis Avulsos de Zoologia* **48:** 247–261.

Matzke NJ. 2013. *BioGeoBEARS: biogeography with Bayesian (and likelihood) evolutionary analysis in R scripts. R Package, Version 0.2, 1. 2013*. https://cran.r-project.org/web/packages/BioGeoBEARS/index.html

Menin M, **Rodrigues DJ**, **Lima AP. 2007.** Clutches, tadpoles and advertisement calls of *Synapturanus mirandaribeiroi* and *S.* cf. *salseri* in Central Amazonia, Brazil. *Herpetological Journal* **17:** 86–91.

Monaghan MT, **Wild R**, **Elliot M**, **Fujisawa T**, **Balke M**, **Inward DJ**, **Lees DC**, **Ranaivosolo R**, **Eggleton P**, **Barraclough TG**, **Vogler AP. 2009.** Accelerated species inventory on Madagascar using coalescent-based models of species delineation. *Systematic Biology* **58:** 298–311.

Motta J, **Menin M**, **Almeida AP**, **Hrbek T**, **Farias IP. 2018.** When the unknown lives next door: a study of central Amazonian anurofauna. *Zootaxa* **4438:** 79–104.

Myers N, **Mittermeier RA**, **Mittermeier CG**, **da Fonseca GAB**, **Kent J. 2000.** Biodiversity hotspots for conservation priorities. *Nature* **403:** 853–858.

Neckel-Oliveira S, **Gordo M. 2004.** Anfíbios, lagartos e serpentes do Parque Nacional do Jaú. In: Borges HS, Iwanaga S, Durigan CC, Pinheiro MR, eds. *Janelas para a Biodiversidade no Parque Nacional do Jaú: uma estratégia para o estudo da biodiversidade na Amazônia*. Manaus: Fundação Vitória Amazônica, 161–176.

Nelson CE, **Lescure J. 1975.** The taxonomy and distribution of *Myersiella* and *Synapturanus* (Anura: Microhylidae). *Herpetologica* **31:** 389–397.

Nomura F, **Rossa-Feres DC**, **Langeani F. 2009.** Burrowing behavior of *Dermatonotus muelleri* (Anura, Microhylidae) with reference to the origin of the burrowing behavior of Anura. *Journal of Ethology* **27:** 195–201.

Olson DM, **Dinerstein E**, **Wikramanayake ED**, **Burgess ND**, **Powell GV**, **Underwood EC**, **D'amico JA**, **Itoua I**, **Strand HE**, **Morrison JC**, **Loucks CJ**, Allnutt TF, Ricketts TH, Kura Y, Lamoreux JF, Wettengel WW, Hedao P, Kassem KR. **2001.** Terrestrial ecoregions of the world: a new map of life on Earth: a new global map of terrestrial ecoregions provides an innovative tool for conserving biodiversity. *BioScience* **51:** 933–938.

Ortiz DA. 2018. *Synapturanus rabus*. In: Ron SR, Merino-Viteri A, Ortiz DA, eds. *Anfibios del Ecuador. Versión 2019.0*. Museo de Zoología, Pontificia Universidad Católica del Ecuador. Accessed 11 April 2020. https://bioweb.bio/faunaweb/amphibiaweb/FichaEspecie/Synapturanus%20rabus

Padial JM, **Miralles A**, **De la Riva I**, **Vences M. 2010.** The integrative future of taxonomy. *Frontiers in Zoology* **7:** 16.

Paluh DJ, **Stanley EL**, **Blackburn DC. 2020.** Evolution of hyperossification expands skull diversity in frogs. *Proceedings of the National Academy of Sciences of the United States of America* **117:** 8554–8562.

Peloso PLV, **Frost DR**, **Richards SJ**, **Rodrigues MT**, **Donnellan S**, **Matsui M**, **Raxworthy CJ**, **Biju SD**, **Lemmon EM**, **Lemmon AR**, **Wheeler WC. 2016.** The impact of anchored phylogenomics and taxon sampling on phylogenetic inference in narrow-mouthed frogs (Anura, Microhylidae). *Cladistics* **32:** 113–140.

Pinheiro PDP, **Kok PJR**, **Noonan BP**, **Means DB**, **Haddad CFB**, **Faivovich J. 2019.** A new genus of Cophomantini, with comments on the taxonomic status of *Boana liliae* (Anura: Hylidae). *Zoological Journal of the Linnean Society* **185:** 226–245.

Pirani RM, **Peloso PLV**, **Prado JR**, **Polo ÉM**, **Knowles L**, **Ron SR**, **Rodrigues MT**, **Sturaro M**, **Werneck FP. 2020.** Diversification history of clown tree frog in Neotropical rainforests (Anura, Hylidae, *Dendropsophus leucophyllatus* group). *Molecular Phylogenetics and Evolution* **150:** 106877.

Pons J, **Barraclough TG**, **Gomez-Zurita J**, **Cardoso A**, **Duran DP**, **Hazell S**, **Kamoun S**, **Sumlin WD**, **Vogler AP. 2006.** Sequence-based species delimitation for the DNA taxonomy of undescribed insects. *Systematic Biology* **55:** 595–609.

Puillandre N, **Lambert A**, **Brouillet S**, **Achaz G. 2012.** ABGD, Automatic Barcode Gap Discovery for primary species delimitation. *Molecular Ecology* **21:** 1864–1877.

Pyburn WF. 1975. A new species of microhylid frog of the genus *Synapturanus* from southeastern Colombia. *Herpetologica* **31:** 439–443.

Pyburn WF. 1977 '1976'. A new fossorial frog from the Colombian rainforest (Anura: Microhylidae). *Herpetologica* **32:** 367–370.

Pyron RA, **Wiens JJ. 2011.** A large-scale phylogeny of Amphibia including over 2800 species, and a revised classification of extant frogs, salamanders, and caecilians. *Molecular Phylogenetics and Evolution* **61:** 543–583.

Quesada CA, **Lloyd J**, **Anderson LO**, **Fyllas NM**, **Schwarz M**, **Czimczik CI. 2011.** Soils of Amazonia with particular reference to the RAINFOR sites. *Biogeosciences* **8:** 1415–1440.

R Core Team. 2016. R: a language and environment for statistical computing. R Foundation for Statistical Computing, Vienna, Austria.

Read M. 2000. *Frogs of the Ecuadorian Amazon, a guide to their calls*. Compact Disk. Fowey, Cornwall, UK: Morley Read Productions.

Ree RH, **Sanmartín I. 2018.** Conceptual and statistical problems with the DEC+J model of founder-event speciation and its comparison with DEC via model selection. *Journal of Biogeography* **45:** 741–749.

Ree RH, **Smith SA. 2008.** Maximum likelihood inference of geographic range evolution by dispersal, local extinction, and cladogenesis. *Systematic Biology* **57:** 4–14.

Réjaud A, **Rodrigues MT**, **Crawford AJ**, **Castroviejo-Fisher S**, **Jaramillo AF**, **Chaparro JC**, **Glaw F**, **Gagliardi-Urrutia G**, **Moravec J**, **De la Riva IJ**, **Perez P**, **Lima AP**, **Werneck FP**, **Hrbek T**, **Ron SR**, **Ernst R**, **Kok PJR**, **Driskell A**, **Chave J**, **Fouquet A. 2020.** Historical biogeography identifies a possible role of the Pebas system in the diversification of the Amazonian rocket frogs (Aromobatidae: *Allobates*). *Journal of Biogeography* **47:** 2472–2482.

Revell LJ. 2012. phytools: an R package for phylogenetic comparative biology (and other things). *Methods in Ecology and Evolution* **3:** 217–223.

Ricklefs RE, **Miles DB. 1994.** Ecological and evolutionary inferences from morphology: an ecological perspective. In: Wainwright PC, Reilly SM, eds. *Ecological morphology: integrative organismal biology*. Chicago: University of Chicago Press, 13–41.

Rivero JA. 1968 '1967'. A new race of *Otophryne robusta* Boulenger (Amphibia, Salientia) from the Chimanta-Tepui of Venezuela. *Caribbean Journal of Science* **7:** 155–158.

Rohlf FJ, **Slice DE. 1990.** Extensions of the Procrustes method for the optimal superimposition of landmarks. *Systematic Biology* **39:** 40–59.

Rojas RR, **Fouquet A**, **Ron SR**, **Hernández-Ruz EJ**, **Melo-Sampaio PR**, **Chaparro JC**, **Vogt RC**, **de Carvalho VT**, **Pinheiro LC**, **Avila RW**, **Farias IP**, **Gordo M**, **Hrbek T. 2018.** A Pan-Amazonian species delimitation: high species diversity within the genus *Amazophrynella* (Anura: Bufonidae). *PeerJ* **6:** e4941.

Ronquist F. 1997. Dispersal-vicariance analysis: a new approach to the quantification of historical biogeography. *Systematic Biology* **46:** 195–203.

Rull V, **Vegas-Vilarrúbia T. 2020.** The Pantepui "Lost World": towards a biogeographical, ecological and evolutionary synthesis of a pristine Neotropical sky-island archipelago. In: Rull V, Carnaval AC, eds. *Neotropical diversification: patterns and processes. Fascinating life sciences*. Cham: Springer, 369–413.

de Sá RO, **Streicher JW**, **Sekonyela R**, **Forlani MC**, **Loader SP**, **Greenbaum E**, **Richards S**, **Haddad CFB. 2012.** Molecular phylogeny of microhylid frogs (Anura: Microhylidae) with emphasis on relationships among New World genera. *BMC Evolutionary Biology* **12:** 241.

San Mauro D, **Gower DJ**, **Müller H**, **Loader SP**, **Zardoya R**, **Nussbaum RA**, **Wilkinson M. 2014.** Life-history evolution and mitogenomic phylogeny of caecilian amphibians. *Molecular Phylogenetics and Evolution* **73:** 177–189.

Schlager S. 2013. *Soft-tissue reconstruction of the human nose: population differences and sexual dimorphism*. Unpublished PhD Thesis, Universitätsbibliothek Freiburg.

da Silva SM, **Townsend PA**, **Carneiro L**, **Burlamaqui TCT**, **Ribas CC**, **Sousa-Neves T**, **Miranda LS**, **Fernandes AM**, **D'horta FM**, **Araújo-Silva LE**, **Batista R**, **Bandeira CHMM**, **Dantas SM**, **Ferreira M**, **Martins DM**, **Oliveira J**, **Rocha TC**, **Sardelli CH**, **Thom G**, **Rêgo PS**, **Santos MP**, **Sequeira F**, **Vallinoto M**, **Aleixo A. 2019.** A dynamic continental moisture gradient drove Amazonian bird diversification. *Science Advances* **5:** eaat5752.

Smith BT, **McCormack JE**, **Cuervo AM**, **Hickerson MJ**, **Aleixo A**, **Cadena CD**, **Perez-Eman J**, **Burney CW**, **Xie X**, **Harvey MG**, **Faircloth BC. 2014.** The drivers of tropical speciation. *Nature* **515:** 406–409.

Stamatakis A. 2014. RAxML version 8: a tool for phylogenetic analysis and post-analysis of large phylogenies. *Bioinformatics* **30:** 1312–1313.

Strauss RE. 1985. Evolutionary allometry and variation in body form in the South American catfish genus *Corydoras* (Callichthyidae). *Systematic Biology* **34:** 381–396.

Streicher JW, **Loader SP**, **Varela-Jaramillo A**, **Montoya P**, **de Sá RO. 2020.** Analysis of ultraconserved elements supports African origins of narrow-mouthed frogs. *Molecular Phylogenetics and Evolution* **146:** 106771.

Trueb L, **Diaz R**, **Blackburn DC. 2011.** Osteology and chondrocranial morphology of *Gastrophryne carolinensis* (Anura: Microhylidae), with a review of the osteological diversity of New World microhylids. *Phyllomedusa* **10:** 99–135.

Tu N, **Yang M**, **Liang D**, **Zhang P. 2018.** A large-scale phylogeny of Microhylidae inferred from a combined dataset of 121 genes and 427 taxa. *Molecular Phylogenetics and Evolution* **126:** 85–91.

Vacher J-P, **Chave J**, **Ficetola FG**, **Sommeria-Klein G**, **Tao S**, **Thébaud C**, **Blanc M**, **Camacho A**, **Cassimiro J**, **Colston TJ**, **Dewynter M**, **Ernst R**, **Gaucher P**, **Gomes JO**, **Jairam R**, **Kok PJR**, **Lima JD**, **Martinez Q**, **Marty C**, **Noonan BP**, **Nunes PMS**, **Ouboter P**, **Recoder R**, **Rodrigues MT**, **Snyder A**, **Marques-Souza S**, **Fouquet A. 2020.** Large scale DNA-based survey of frogs in Amazonia

suggests a vast underestimation of species richness and endemism. *Journal of Biogeography* **47:** 1781–1791.

Vacher J-P, **Kok PJR**, **Rodrigues MT**, **Lima JD**, **Lorenzini A**, **Martinez Q**, **Fallet M**, **Courtois EA**, **Blanc M**, **Gaucher P**, **Dewynter M**, **Jairam R**, **Ouboter P**, **Thébaud C**, **Fouquet A. 2017.** Cryptic diversity in Amazonian frogs: integrative taxonomy of the genus *Anomaloglossus* (Amphibia: Anura: Aromobatidae) reveals a unique case of diversification within the Guiana Shield. *Molecular Phylogenetics and Evolution* **112:** 158–173.

Vidal-García M, **Keogh JS. 2017.** Phylogenetic conservatism in skulls and evolutionary lability in limbs – morphological evolution across an ancient frog radiation is shaped by diet, locomotion and burrowing. *BMC Evolutionary Biology* **17:** 165.

Vieites DR, **Wollenberg KC**, **Andreone F**, **Köhler J**, **Glaw F**, **Vences M. 2009.** Vast underestimation of Madagascar's biodiversity evidenced by an integrative amphibian inventory. *Proceedings of the National Academy of Sciences of the United States of America* **106:** 8267–8272.

Wallace AR. 1854. On the monkeys of the Amazon. *Annals and Magazine of Natural History* **14:** 451–454.

Wassersug RJ, **Pyburn WF. 1987.** The biology of the Pe-Ret' toad, *Otophryne robusta* (Microhylidae), with special consideration of its fossorial larva and systematic relationships. *Zoological Journal of the Linnean Society* **91:** 137–169.

Wild ER. 1995. New genus and species of Amazonian microhylid frog with a phylogenetic analysis of New World genera. *Copeia* **1995:** 837–849.

Wilkinson M. 1995. Coping with abundant missing entries in phylogenetic inference using parsimony. *Systematic Biology* **44:** 501–514.

Zweifel RG. 1986. A new genus and species of microhylid frog from the Cerro de la Neblina region of Venezuela and a discussion of relationships among New World microhylid genera. *American Museum Novitates* **2863:** 1–24.

SUPPORTING INFORMATION

Appendix S1. Additional information on methods.

Appendix S2. Justifications for confirmed/unconfirmed candidate species status.

Table S1. Sample details, data (morphological, acoustical, molecular) are summarized in the grey coloured cells on the right. Collections: Colección de Anfibios y Reptiles de la Universidad de Nariño (PSO-CZ); American Museum of Natural History (AMNH); Royal Ontario Museum (ROM); University of Texas (UTA); Smithsonian Institution (USNM); Museu de Ciências e Tecnologia da PUCRS (MCP); Musée National d'Histoire Naturelle Reptiles Amphibiens (MNHN-RA); Instituto Nacional de Pesquisas da Amazônia (INPA); Museu Paraense Emílio Goeldi (MPEG); State Museum of Natural History Stuttgart (SMNS); Museu de Zoologia da Universidade de São Paulo (MZUSP, CTMZ), Colección Referencial de Biodiversidad del Instituto de Investigaciones de la Amazonía Peruana (CRBIIAP); Museo de Zoologia de la Universidad Nacional de la Amazonia Peruana (MZUNAP); Museo de Historia Natural La Salle (MHNLS); Museo de Zoologia de la Pontificia Universidad Catolica del Ecuador (QCAZ); Museum für Tierkunde, Senckenberg Naturhistorische Sammlungen (MTD); Institut royal des Sciences naturelles de Belgique (IRSNB). Field numbers acronyms are: AF=Antoine Fouquet, MTR=Miguel Trefaut Rodrigues, PK= Philippe Kok, CM=Christian Marty, PG= Phillipe Gaucher, RE= Raffael Ernst, ST=Jucivaldo Lima, SCF= Santiago Castroviejo Fisher, DT=Dante Pavan, BPN= Brice P. Noonan, RWM=Ross McCulloch, MW= Mark Wikinson, GGU=Giussepe Gagliardi Urrutia, AJC=Andrew J. Crawford.

Table S2. Primer details.

Table S3. External morphometric data for *Synapturanus*. Criteria used to identify specimens (genotypes, same population as genotyped specimens, etc.) are indicated in the second column.

Table S4. Acoustic data for *Synapturanus* spp. Criteria used to identify specimens (genotypes, same population as genotyped specimens, etc.) are indicated in the fifth column. Variables are note length (NL), dominant frequency (DoF), number of pulses per note and delta frequency (DeF). Repository where records are available are indicated in the right column.

Table S5. Chimeric data assembly for molecular dating.

Table S6. Micro-computed tomography scan data (species, voucher, sex and data source.

Table S7. Traits considered for ecological categorization of the species included in the morphological analyses.

Table S8. Mean pairwise distances (p-dist, pairwise deletion) based on 577 bp of the 16S gene; SD (in blue) estimated via 100 bootstraps.

Table S9. Results from principal components analysis of external morphometric data. A, uncorrected morphometric data. B, size-corrected data (residuals).

Table S10. Results from the principal components analysis of acoustic data.

Table S11. Species delimitation results, conflicting delimitation and the *Otophryne pyburni* terminal added are highlighted in red.

Table S12. BIOGEOBEARS model estimates. The model column lists the different models compared with BIOGEOBEARS. The log likelihood for each model is in the Lnl column. Best fit of the anagenetic dispersal, extinction and founder event parameters are found respectively in columns d, e and j. The Akaike information criterion is given in the AIC column.
Figure S1. Maximum likelihood tree obtained using RAXML with a GRT+I+Γ model (1000 bootstrap replicates) on the three concatenated nuclear DNA loci.
Figure S2. Landmarks of cranium (A) and humerus (B).
Figure S3. Complete maximum clade credibility chronogram obtained from the analysis of 16S (577 bp) using BEAST.
Figure S4. Results from principal components analysis (PCA) of external morphometric data. Top, PCA using uncorrected external morphological data: PC1 × PC2 (also in the main text) and PC2 × PC3. Bottom, PCA using residuals of the regression of each variable on snout–vent length (SVL). Contribution of variables and eigenvalues of PCs are depicted in the left-hand graphs.
Figure S5. Results from BIOGEOBEARS with the DIVA model.
Figure S6. A, B, cranial and humeral shape variation with full labels (see Fig. 4). C, two-block partial least squares analysis (2B-PLS) with all Microhylidae.
Figure S7. Main types of soils from the Soil and Terrain Database for Latin America and the Caribbean data (SOTERLAC) in the focal area and Synapturanus occurrences coloured according to their phenotypes (boundaries represented by white polygons). The limits of Amazonia are depicted in red.

SHARED DATA

The data used in all analyses have been deposited in online repositories: GeneBank (molecular data), Morphosource (uCT-Scans) and in "La sonothèque du muséum national d'histoire naturelle" (acoustic data); or are directly available in supporting information files.